NASA TECHNICAL MEMORANDUM

NASA TM X-62,337

NASA TM X-62,337

A REVIEW OF TURBULENCE MEASUREMENTS IN COMPRESSIBLE FLOW

V. A. Sandborn

Ames Research Center
Moffett Field, Calif. 94035

March 1974

A REVIEW OF TURBULENCE MEASUREMENTS IN COMPRESSIBLE FLOW

By

V. A. Sandborn

A survey of turbulence measurements in compressible flows is presented. The majority of turbulence measurements at super- and hypersonic speeds have been made for the zero pressure gradient, turbulent boundary layer. It was found that the nondimensional turbulent stress terms for the zero pressure gradient flow appear to agree closely with equivalent incompressible measurements in the outer part of the boundary layer. The stress terms were nondimensionalized by the wall value of shear stress and plotted versus the distance from the wall, nondimensionalized by the boundary-layer thickness. Indirect evaluation of the total shear stress distribution from mean velocity measurements for both super- and hypersonic flows (zero pressure gradient, two-dimensional flows) indicate a near universal distribution. These total shear stress curves also agree very closely with measured incompressible shear stress distributions. Recent laser anemometer measurements of the turbulent Reynolds shear stress ($\rho\overline{uv}$), reported by Johnson and Rose for a Mach number 2.9 flow, are in reasonable agreement with the expected total shear stress curve over the outer 60% of the boundary layer. Near the surface a systematic deviation between the laser measurements and expected shear stress was found. The laser anemometer data are only slightly higher than the incompressible results for the individual longitudinal and vertical turbulent velocity components over the complete boundary layer. These results might be taken to suggest, with some reservation, that the term ($\rho\overline{uv}$) may not be the only important term in the turbulent shear stress for supersonic boundary layers.

Hot-wire anemometer measurements of the longitudinal component of the turbulent velocity in super- and hypersonic flow were found to agree with the incompressible data in the outer region of the layers. Measurements of the vertical component of the turbulent velocity and the Reynolds shear stress with hot wires appear questionable. Mass flux and temperature fluctuation measurements show considerable scatter from one boundary layer to another. Neither mass flux or temperature data could be correlated with the degree of similarity observed for the turbulent stress terms.

The spectral energy distribution of the super- and hypersonic flows are also shown to correspond to equivalent incompressible results. The spectral curves may be used to specify the frequency range of interest for a given boundary-layer measurement. Intermittency of the outer edge of the super- and hypersonic boundary layers is markedly different from that of the incompressible layer.

Reported measurements of the free-stream mass flux intensity were found to increase as the square of the Mach number for both the super- and hypersonic wind tunnels. Very few measurements for subsonic compressible flow have been reported. A limited number of data points for the turbulent shear stress in a subsonic, compressible, pipe flow were found.

INTRODUCTION

Techniques of dealing with turbulent shear flows are limited due to a lack of a rational theory of turbulent flow. Engineering calculations of flow about bodies still rely heavily on empirical information about the turbulence. Thus, it is necessary to experimentally evaluate turbulent shear flows, in order to upgrade and check the analytical methods.

Measurements of turbulent properties in compressible flows have proven quite difficult. Although the basic concepts of measuring turbulence with hot-wire anemometers in compressible flows were evolved by Kovasznay, ref. 1 and 2, in the early fifties, very few measurements were reported. In the late fifties a limited number of surveys by Morkovin and Phinney, ref. 3, and by Kistler, ref. 4, for supersonic boundary layers were reported. Only within the last few years have further measurements of compressible turbulence appeared. All the measurements are limited in content, so that it is difficult to access the accuracy of any one set of data.

The present paper was undertaken as a comprehensive survey of compressible turbulence. In 1962 Morkovin, ref. 5, reviewed the effects of compressibility on turbulent flow and proposed limited guidelines as to expected effects. Morkovin showed that the effects of compressibility were expected to be somewhat passive. Based on the observations of Morkovin, together with recent observations of large Reynolds number similarity of incompressible turbulent boundary layers, it was possible to examine in surprising detail a great amount of compressible turbulence data. The present survey is mainly limited to the simple flat plate boundary layer. However, it should serve as a guide to the evaluation of measuring techniques for studies of more complex flows.

SYMBOLS

A	supersonic tunnel geometry constant, eq. (8)
e	hot wire anemometer voltage fluctuation
E	total energy
E'	fluctuating part of the total energy
f	frequency
$F(k)$	wave number spectral energy function, eq. (15)
k	wave number
L_x	macroscale of the longitudinal turbulent velocity component in the x-direction, eq. (16)
M	Mach number
p	static pressure
p'	fluctuating part of the static pressure
Pr	Prandtl number
r	radial coordinate
Re	Reynolds number
R_θ	Reynolds number based on the boundary-layer momentum thickness
R_{mT}	correlation between the mass flow and temperature fluctuations
R_x	correlation of the longitudinal turbulent velocity components in the x-direction
$R_{\sigma\tau}$	correlation between the entropy and vorticity fluctuations.
q_t	turbulent heat flux
T	temperature
T'	fluctuating part of the temperature
u	x-direction turbulent velocity component
U	x-direction mean velocity component
U_τ	shear stress velocity $(\sqrt{\tau_w/\rho})$

v	y-direction turbulent velocity component
V	y-direction mean velocity component
w	z-direction turbulent velocity component
x	longitudinal coordinate in direction of the mean flow
y	vertical coordinate in direction perpendicular to the mean flow and to the surface (for boundary layers)
y^*	nondimensional vertical coordinate (yU_τ/ν)
z	horizontal coordinate in direction perpendicular to the mean flow and parallel to the surface (for boundary layers)
γ	intermittency factor (percent of time turbulent)
δ	boundary-layer thickness
λ_x	microscale of the longitudinal turbulent velocity component
ρ	fluid density
ρ'	fluctuating part of the fluid density
τ	shear stress
τ_t	turbulent shear stress
τ_w	wall shear stress
μ	coefficient of viscosity
ν	kinematic viscosity

Subscripts

1	initial conditions
e	edge of shear flow
f	at the specific frequency f
o	total temperature
r	recovery temperature
t	turbulent part
w	wall value

General Requirements for Turbulent Measurements in Compressible Flows

Major interests in turbulent measurements arise from the need to evaluate flows about bodies, and in their wakes. These flows can be classified as turbulent shear flows. Other areas of interest include regions of turbulent mixing, as associated with problems such as jet engines and combustion processes. Also, since most aerodynamic studies are carried out in wind tunnels, a good deal of effort has been expended to evaluate the free-stream turbulence level of supersonic wind tunnels. Examination of the equations governing compressible, turbulent, flow will give an indication of the important turbulent quantities that need to be determined.

Detailed derivations of the compressible equations are given by Van Driest, ref. 6, and by Schubauer and Tchen, ref. 7. For the present survey of compressible turbulence measurements it was found to be adequate to employ only the boundary-layer approximations of the complete equations. Following the analysis of Schubauer and Tchen, the steady-state boundary-layer equations may be written as:

MOMENTUM

$$\frac{\partial}{\partial x}(\bar{\rho}\bar{U}^2) + \frac{\partial}{\partial y}(\bar{\rho}\bar{U}\bar{V}) = \frac{\partial \bar{p}}{\partial x} + \frac{\partial}{\partial y}\left[\mu\frac{\partial U}{\partial y} - \tau_t - U\overline{\rho' v}\right] \tag{1}$$

$$\frac{\partial \bar{p}}{\partial y} + \frac{\partial}{\partial y}(\bar{\rho}\,\overline{v^2}) = 0 \tag{2}$$

CONTINUITY

$$\frac{\partial}{\partial x}(\bar{\rho}\bar{U}) + \frac{\partial}{\partial y}(\bar{\rho}\bar{V} - \overline{\rho' v}) = 0 \tag{3}$$

ENERGY

$$\frac{\partial}{\partial x}(\bar{\rho}\bar{E}\bar{U}) + \frac{\partial}{\partial y}(\bar{\rho}\bar{E}\bar{V}) = \frac{\partial}{\partial y}(\frac{\partial \bar{E}}{\partial y} - q_t) + \frac{\partial}{\partial y}(\frac{1}{Pr} - 1)\mu\frac{\partial C_p \bar{T}}{\partial y}$$

Schubauer and Tchen argue that the turbulent shear stress, τ_t, is just equal to $\overline{\rho uv}$, which is equivalent to the incompressible results. Van Driest employs a slightly different approach wherein $U\,\overline{\rho' v}$ remains lumped with the corresponding inertia term. The turbulent shear stress, τ_t, for Van Driest's analysis is given as

$$\tau_t \equiv -\overline{(\rho v')u} = -\bar{\rho}\,\overline{uv} - V\overline{\rho' u} - \overline{\rho' uv} \qquad (5)$$

It should be noted that evaluation of the total or turbulent shear stress from mean flow measurements, assuming similarity, produces a value equivalent to that of equation (5). Schubauer and Tchen neglect all but $\bar{\rho}\,\overline{uv}$.

From the equations it is found that the following turbulence quantities should be specified.

MOMENTUM $\overline{uv}$, $\overline{v^2}$, $\overline{\rho' v}$, $\overline{\rho' u}$, $\overline{\rho' uv}$

ENERGY $(q_t =) -\overline{(\rho v)' E'} = -\bar{\rho}\,\overline{vE'} - V\overline{\rho' E'} - \overline{\rho' vE'}$

Not all of these terms have been measured, nor can their magnitudes be estimated from the existing data.

As is well known, equations (1) through (4) are not a closed set, due to the addition of the turbulence terms. Thus, the analytical evaluation must depend on some independent knowledge of the turbulence quantities. In particular, the shear stress and the heat flux terms are of major importance for engineering

predictions. For most boundary-layer flows it is found that the y-direction momentum equation, eq. (2), is independent of the x-direction equation, eq. (1). Thus, equation (2) can be integrated directly to give

$$\overline{\rho}\,\overline{v^2} = (\overline{p} - \overline{p}_e) \tag{6}$$

If $\overline{v^2}$ is small, then the variation of static pressure, $\overline{p}$, across the shear layer can be neglected.

For the boundary-layer evaluations that are considered later the vertical mass flux, $\overline{\rho' v}$, is lumped directly with $\overline{\rho}V$. Direct measurements of $\overline{\rho' v}$ do not appear to have been successful, so very little is known about its magnitude. Indirectly, $\overline{\rho' v}$, could be evaluated from the continuity equation, eq. (3), by measuring the derivatives of the mean mass fluxes (for steady flow, $\frac{\partial \overline{\rho}}{\partial t} = 0$)

$$\overline{\rho' v} = -\int_0^y \left[\frac{\partial}{\partial x}(\overline{\rho}U) - \frac{\partial}{\partial y}(\overline{\rho}V)\right] dy \tag{7}$$

The major interest in compressible turbulent boundary layers will be the evaluation of the shear stress. A number of measurements of $\overline{\rho}\,\overline{uv}$ have been reported within the last year. Also, a large number of indirect evaluations of the shear stress from mean flow measurements have been reported for a wide range of super- and hypersonic boundary layers. For the case of zero pressure gradient, turbulent boundary layers, a surprisingly good agreement between the mean flow evaluations of turbulent shear stress was found in the course of the present survey.

The basic equations of motion and energy are insensitive to much of the turbulent fluctuations. As a result, it has been necessary to seek higher order turbulent energy equations, ref. 8, in order to explore the "turbulent structure." These higher order turbulent energy equations have been employed in recent years as model equations to determine the turbulent shear stress, $\overline{uv}$. Unfortunately, the assumptions necessary to deal with the higher order turbulent terms introduce a new set of uncertainties. Due to the difficulties in measuring turbulence in compressible flows, it is doubtful that experimental evaluation of the higher order turbulent energy equations is feasible.

Although, not necessarily part of the solution of the equations governing turbulent shear flows, a large number of turbulent momentum and energy terms can be considered.

MOMENTUM			ENERGY
Turbulent Shear	Mass Flow	Triple Correlation	
$\overline{\rho}\,\overline{u^2}$	$V(\overline{\rho u})'$	$\overline{\rho' uv}$	
$\overline{\rho}\,\overline{v^2}$	$U(\overline{\rho v})'$	$\overline{\rho' uw}$	$\overline{\rho}\,\overline{v\,E'}$
$\overline{\rho}\,\overline{w^2}$	$U(\overline{\rho w})'$	$\overline{\rho' vw}$	$V\,\overline{\rho' E'}$
$\overline{\rho}\,\overline{uv}$			$\overline{\rho' vE'}$
$\overline{\rho}\,\overline{uw}$			
$\overline{\rho}\,\overline{vw}$			

where u, v and w are the three turbulent velocity components. As previously noted, some of these terms are important in the equations, while others appear

as derivatives that can be neglected. For a large number of turbulent flows of importance a quasi-symmetry, either plane or cylindrical, can be obtained by proper choice of coordinates, so that the cross-velocity correlations, $\overline{uw}$ and $\overline{vw}$ (or $\overline{uv}$ depending on the coordinates chosen), can be neglected. These cross products will be zero if no shear exists in the z (or w) direction.

The mass flux terms are of particular interest in evaluating the free-stream conditions of the compressible flow wind tunnels. Turbulent density and temperature fluctuations are also of interest in free-stream evaluations. In supersonic hot-wire anemometry evaluations the density fluctuations are directly coupled with the velocity fluctuations. Thus, it is found necessary to relate the independent temperature fluctuation measurements to the density. The relation between density and temperature fluctuations requires some knowledge as to the pressure fluctuations, since they are coupled through the equation of state. Thus, for most measurements the pressure fluctuations are assumed to be neglectable, and the density is related directly to the temperature. Independent measurements of the pressure fluctuations within the boundary layer are desirable, but experimental methods have not been available to measure them other than at the surface. A great deal of information has been obtained on the basic structure aspects of the turbulent fluctuations, such as:

(a) energy-frequency content

(b) probability distributions

(c) correlations and related quantities such as scales and convective velocities.

REPORTED TURBULENCE MEASUREMENTS

A general review of existing measurements of turbulence in compressible flows has been made. The review both demonstrates what turbulent quantities can be measured, and the areas where information is available. At the present time it appears that very little information exists for the area of subsonic compressible flow. In some areas, such as zero pressure gradient, supersonic, turbulent boundary layers, a great deal of information is available. The present section is divided into four parts, according to the particular flow:

(a) Free-stream Turbulence

(b) Fully Developed Pipe Flow

(c) Boundary Layers

(d) Free Shear Flow

(a) Free-stream Turbulence.- Historically, a good deal of effort was expended in the mid-nineteen fifties to evaluate the free-stream turbulence level of supersonic wind tunnels. An early NACA attempt to compare the turbulence level of different supersonic wind tunnels consisted of measuring the transition location on a "standard" 10° cone, ref. 9. The transition was determined by measuring the recovery temperature distribution along the cone. Similar type studies have more recently, ref. 10, 11 and 12, been evaluated in the hypersonic facilities. Fischer and Wagner, ref. 10, obtained correlation curves of transition Reynolds number versus the free-stream disturbance levels for $M_e \geq 5$ at the edge of the boundary layer. The transition Reynolds number was found to vary approximately as the inverse of the free-stream, mass flow fluctuation (or sound disturbance level) for a constant Mach number. An examination of the

limited measurements reported by Sandborn and Wisniewski, ref. 13, for the NACA, "standard" 10° cone in a small, 6- by 6-inch, Mach number 3 wind tunnel indicates a similar linear inverse relation. Note that it is necessary to separate the Mach number and turbulence level effects before different tunnels are compared.

Figure 1 is a plot of the mass flow fluctuation intensity versus Mach number reported by a number of experimenters. For Mach numbers below 2, Laufer, ref. 14, and Morkovin, ref. 13, found that the velocity fluctuations upstream of the sonic throat affects the free-stream turbulence in the supersonic flow. At a Mach number of approximately 2.5 the upstream velocity fluctuations could no longer be related to the test section turbulence. For a Mach number range from 1.6 to 5, Laufer, ref. 16, found from hot-wire measurements that the correlation coefficient between mass flow and total temperature fluctuations in the free-stream had values of approximately -1. Secondly, it was known that neither static temperature nor velocity fluctuations by themselves were sufficient to produce the high turbulence levels indicated by the hot wire. Based on the analysis of Kovasznay, ref. 2, it was apparent that the only simple fluctuating field consistent with the measurements was a pure sound field. For a pure sound field the isentropic relations between pressure, density and temperature (and their fluctuations) are valid. Evidence for sound domination of the supersonic free-stream has been reported for a number of facilities. The sound fluctuations are related directly to the mass flow fluctuations measured with the hot-wire anemometer. The only deviations appear in the hypersonic flow facilities, where inlet flows must be heated to high temperatures. For the hypersonic facilities, ref. 11 and 17, large temperature, as well as mass flow fluctuations are encountered.

The measurements of Laufer, ref. 16, Sandborn and Wisniewski, ref. 13, and Donaldson and Wallace, ref. 18, all show that the mass flow fluctuation intensity decreases with increasing Reynolds number at a fixed Mach number. The decrease is estimated to vary as $Re^{-.25}$. It was pointed out by Laufer, ref. 16, that the wall boundary layers, which generate the freestream sound fluctuations, become thinner as the Reynolds number increases. The wall boundary-layer effect was dramatically demonstrated by Laufer, ref. 16, by reducing the tunnel Reynolds number to where the wall layers are laminar. The point shown on figure 1 at $M = 4.5$ (Laufer, $Re/in = 2.6 \times 10^4$) shows almost an order-of-magnitude reduction in tunnel mass-flow fluctuations. Although the data of figure 1 fail to agree in all cases there is evidence to suggest that the larger size supersonic wind tunnels for a given Mach number will have the lower turbulence levels ($M > 2$). The ratio of free-stream area to boundary-layer perimeter should be an important parameter.

The increase of the mass-flow fluctuation intensity with Mach number is a result of the sound field being proportional to the fourth power of the Mach number, ref. 16. A curve fit of the data of Laufer for $M > 2$ shows that the actual mass-flow fluctuations increase as M^2. As an approximate curve fit, the following relation was obtained

$$\frac{\overline{(\rho u)'}}{\rho U} = A \, Re_{/in}^{-.25} \, (M^2 - .5) \qquad (8)$$

where the constant A accounts for the variation due to tunnel size (and/or origin of the sound source). For Laufer's data a value $A = 0.0095$ was estimated.

Curves for A = 0.0095 and Re/in = 90,000 and 330,000, corresponding to Laufer's measurements, are plotted on figure 1. A curve for A = 0.017 and Re/in = 90,000 is plotted to demonstrate the effect of A. This latter curve is an approximate fit of the Sandborn-Wisniewski data for the 6- by 6-inch tunnel. The measurements of Kistler, ref. 4 shown on figure 1, may not represent a true value for the wind tunnel, as they were taken at the edge of the wall boundary layer. Kistler reported that the free-stream levels were below the noise level of his measuring system.

The very high Mach number results, shown as the insert on figure 1, do not vary according to equation (8). The particular facility is such that the Mach number increases as the Reynolds number is increased (see ref. 10). Thus, the higher Mach numbers also represent higher Reynolds numbers. Both the variation with Mach number and with Reynolds number are greater than would be predicted by equation (8). Note also that the mass flow intensities are much lower than the extrapolation of the supersonic curves, shown on figure 1, would predict.

(b) Quasi-fully Developed Pipe Flow.- Fully developed pipe flow has proven of great value in the evaluation of turbulence measurement techniques for the incompressible case. It is possible that similar results can be obtained for compressible flows. For a compressible subsonic flow there is a progressive decrease in density along the pipe, so that the local velocity must increase with downstream distance. It is,however, found that a quasi-full-developed pipe flow may be obtained. Kjellström and Hedberg, ref. 19, consider the quasi-fully-developed flow momentum equation as

$$\bar{\rho}U\frac{\partial U}{\partial x} = -\frac{dp}{dx} - \frac{1}{r}\frac{\partial}{\partial r}(\tau r) \qquad (9)$$

The shear stress variation with radius becomes

$$\tau = \frac{r}{2}\frac{dp}{dx} + \frac{1}{r}\int_o^r r\overline{\rho U}\frac{\partial U}{\partial x}dr \qquad (10)$$

For incompressible flow the second integral in equation (10) is zero, so that the shear stress varies linearly across the pipe radius. Durst, Launder and Kjellstrom, ref. 20, have evaluated equation (10) for a typical empirical velocity distribution, They find a progressively increasing nonlinearlity due to the velocity term as the Mach number increases from 0.5 to 0.7.

Figure 2 shows the results of an experimental study reported by Gibbings and Mikulla, ref 21, for subsonic, compressible, quasi-fully-developed, pipe flow. Both the shear stress distribution experimentally evaluated from a form of equation (10), and direct hot-wire measurements of $\overline{\rho uv}$ were obtained. The nonlinear, "compressible" effect on the computed total shear stress was evident for a Mach number of 0.51, although it was small. The hot-wire measurements were found to agree with the evaluation of equation (10) over the center region of the pipe. Near the wall the value of $\overline{\rho uv}$ drops to zero somewhat faster than might be expected. These measurements are the only subsonic, compressible, turbulence data found.

(c) Boundary Layers.- The major interest of compressible turbulence measurement studies has been the supersonic boundary layer. A review of the literature showed a number of studies of zero pressure gradient, supersonic, turbulent boundary layers has been made. These studies range in Mach number from 1.7 to 9.4. Temperature and mass flow fluctuations have also been reported for M = 20. No measurements that contain compressible effects at subsonic Mach numbers were

found. Serafine, ref. 22, reports longitudinal turbulent intensity measurements for a M = 0.6 flow, however, all effects of compressibility were neglected.

In the section on general requirements it was noted that the basic turbulent terms required for evaluation of the continuity, momentum and energy equations were: $\overline{uv}$, $\overline{\rho'v}$, $\overline{\rho'u}$,$\overline{\rho'uv}$,$\overline{\rho'E'}$, $\overline{vE'}$ and $\overline{\rho'vE'}$. These quantities have proven very difficult to measure directly with hot-wire anemometers. Figure 3 is a summary plot of measurements of $\rho\overline{uv}$ that have been reported for supersonic, zero pressure gradient, turbulent boundary layers. All of the data on figure 3 have been reported within the current year, so it would appear that major electronic difficulties are not expected. The shaded curve, shown on figure 3, represents a "best estimate" of the total shear stress (viscous plus turbulent, as given by eq. (5)) which will be discussed in more detail in the following paragraph. The measured values of $\rho\overline{uv}$ were obtained with hot wire and laser anemometers. The measurements of Rose and Johnson, ref. 24, with a laser system do not require any assumption regarding the pressure fluctuations. If $\rho\overline{uv}$ were the only term of importance in the compressible turbulent shear stress relation, as is the case for incompressible flow, the laser measurements should agree with the shaded curve shown on figure 3. The laser data agree approximately with the best estimate shear stress distribution over the outer 60% of the layer. Near the surface the systematic deviation of the laser data from the expected results poses a question on the accuracy of the data. While it is difficult to access the accuracy, it will be shown that the evaluation of $\overline{u^2}$ and $\overline{v^2}$ from the same set of data are in reasonable agreement with the incompressible results. Both $\overline{u^2}$ and $\overline{v^2}$ were found to be slightly higher than the corresponding incompressible measurements over most of the boundary layer.

A second possibility for the deviation of the laser measurments (of $\overline{\rho uv}$ from the expected total shear stress curve) is that the other terms in the compressible shear stress, eq. (5), become important near the surface. The viscous term was estimated from the mean velocity measurements, and found to be two orders of magnitude smaller than the measured $\overline{\rho uv}$ term. The turbulent term $V\overline{\rho' u}$ would be expected to be small near the surface, since V is small. A rough estimate based on a linear variation of V, with $(V/U)_e \simeq 0.1$, indicated this term is less than 5% of $\overline{\rho uv}$. Also $V\overline{\rho' u}$ has an opposite sign compared to $\overline{\rho uv}$, so it would act to increase rather than decrease the deviation near the surface. It appears that the deviations occur in the region where the turbulent fluctuation $\sqrt{\overline{v^2}}$ is of the same order of magnitude as the mean vertical velocity component, V. The term $\overline{\rho' uv}$ is generally suggested to be quite small, although there is no direct experimental information available on its magnitude.

Although direct measures of the turbulent shear stress for supersonic boundary layers are not satisfactory, indirect evaluation from the equations of motion appear to give reasonably consistent results. For a zero pressure gradient, steady flow, equation (1) can be solved for the shear stress

$$\tau \equiv \left(\mu\frac{\partial U}{\partial y} - \bar{\rho}\,\overline{uv} - V\overline{\rho' u} - \overline{\rho' uv}\right) = \tau_w + \int_o^y \left\{\frac{\partial}{\partial x}(\bar{\rho}U^2) - \frac{\partial}{\partial y}(\bar{\rho}UV)\right\}dy \qquad (11)$$

It is possible to make sufficient mean flow measurements to evaluate the mean flow derivatives in the integral term. However, for the evaluations that have appeared for equation (11), an assumption of "similarity" was employed. The similarity introduced by Meier and Rotta, ref 25, assumes that the velocity and temperature, or density, profiles in the x-direction are self-similar. Exact similarity for

zero pressure gradient flow requires that the wall shear stress is constant with x, and the boundary-layer thickness vary linear with x. It is experimentally found that the incompressible, zero pressure gradient, boundary layer approaches the similarity requirements at "large" Reynolds numbers, Zoric, ref. 26.

Figure 4 is a summary plot of the total shear stress distributions computed from similarity forms of equation (11). The data shown in the main part of figure 4 are for measurements along flat plates, conical models and on two-dimensional tunnel walls. A wide range of both Mach number and Reynolds number are represented in the data used to compute the distributions shown on figure 4. There are surpisingly only small variations in the diverse number of measurements. The data shown are mainly for near adiabatic flow conditions, although heat transfer is also represented. The data of Horstman and Owen, ref. 27, Danberg, ref. 28, (evaluated by Bushnell and Morris, ref 29) and Samuels, Peterson and Adcock, ref 30, (also evaluated by Bushnell and Morris) are all for wall to freestream temperature ratios of the order of 0.45 to 0.48. Of the data found in the literature only a set of three profiles reported by Rochelle, ref. 31, for M = 2.029, 2.480 and M = 4.975 are not included on figure 4. The profile evaluated by Rochelle for M = 2.480 falls approximately within the limits of those shown on figure 4 (it appears to indicate a decreasing pressure gradient), but the other profiles fall well below the present results. Apparently some question arises in the technique of calculation used in this early evaluation.

A "best estimate" for the shear distribution for two-dimensional zero pressure gradient, supersonic, turbulent boundary layers was constructed

from the curves of figure 4. The "best estimate" distribution is shown on figures 3, 4 (insert) and 5 as the shaded regions. From the equation of motion, eq. (1) the boundary condition for the shear stress at the wall is

$$\left.\frac{\partial \tau}{\partial y}\right|_{y=0} = \left.\frac{\partial p}{\partial x}\right|_{y=0} \tag{12}$$

For a zero pressure gradient the shear distribution must approach the surface with zero slope. Of the distributions shown on figure 4, the profiles of Horstman and Owen, ref. 27 (for $R_\theta = 9.7 \times 10^3$ only) and the one from Danberg, ref. 28, (evaluated by Bushnell and Morris, ref. 29) appear to indicate a negative slope for $\left.\frac{\partial \tau}{\partial y}\right|_{y=0}$. Thus, in drawing the best estimate distribution the region near the wall does not include these two distributions.

The scatter between the profiles in the outer region of the boundary layer may represent an experimental uncertainty in defining the boundary-layer edge. The boundary-layer edge is a statistical property, which is not well defined in the mean-flow measurements. Incompressible measurements, such as those of Klebanoff, ref. 32, for zero-pressure-gradient boundary layers, show that the turbulent shear stress goes to zero at values slightly greater than the statistical boundary-layer edge. At the boundary-layer edge the incompressible turbulent shear stress was approximately two orders of magnitude less than the wall shear stress, as shown on figure 5. It is reasonable to assume that the supersonic shear stress should also approach closely to zero at $y/\delta = 1$.

Several shear stress distributions for boundary layers in nozzle-type flows are shown on the insert of figure 4. It is not at present possible to determine the validity of the similarity concept in the evaluation of these flows.

It is, however, doubtful that the large differences between axisymmetric and two-dimensinnal flows, shown on figure 4, are to be expected.

Between the different sets of measurements represented on figure 4, it was not possible to identify consistent Mach number or Reynolds number variations. The systematic variation of Mach number at constant Reynolds number, reported by Meier and Rotta, ref. 25, appears to show a small systematic increase in the values of τ/τ_w with increasing Mach number for most of the boundary layer. With perhaps the exception of the M = 4.5 data, the variation with Mach number was quite small. Systematic variation of Reynolds number reported by Horstman and Owen, ref. 27, and also Meier and Rotta indicate a slight decrease in the values of τ/τ_w with increasing Reynolds number for most of the boundary layer. The possibility exists that, since all the evaluations employ the similarity approximations, the resulting distribution must be locked to a similarity shape. Obviously, the fixing of the distribution to $\tau/\tau_w = 1$ at $y/\delta = 0$ and $\tau/\tau_w \simeq 0$ at $y/\delta = 1$, together with a zero slope at $y/\delta = 0$, makes large variations unlikely.

For subsonic flow the variation of the zero pressure gradient, turbulent shear distribution from the near-similarity condition to a flow with an order of magnitude smaller Reynolds number is within the accuracy of the measurements. Figure 5 compares the faired incompressible measurements of turbulent shear stress reported by Zoric, ref. 26, for $R_\theta = 42 \times 10^3$ with Klebanoff's data, ref. 32, for $R_\theta = 7.75 \times 10^3$. The flow evaluated by Zoric was very close to the similarity type that is presently assumed in the supersonic shear stress evaluations. The comparison of the incompressible measurements appears to

support the use of the similarity assumptions to evaluate the turbulent shear stress. The incompressible measurements might well represent the lower limit of the "best estimate" distribution.

Maise and McDonald, ref. 33, have derived shear stress distributions based on an empirical correlation of measured boundary layer, mean velocity profiles. Their predicted shear distribution for $M = 5$ is shown on figure 5. The empirical distribution is higher than the experimental evaluations over most of the layer. A similar over-prediction of the incompressible shear distribution is also noted in their results. The analysis does, however, predicte a small increase in the shear stress as Mach number increases, and also a small decrease in shear stress as Reynolds number increases.

In summary it may be proposed that measurements of the turbulent shear stress, $(-\rho\overline{uv} - \overline{\rho' uv} - V\overline{\rho' u})$, for supersonic, zero pressure gradient, two-dimensional, adiabatic, turbulent boundary layers should fall within the "best estimate" curve, shown on figure 3. The exception, of course, is the region very close to the surface where the turbulent shear stress must drop to zero. The zero pressure gradient flow should serve as a check of the turbulence measuring technique.

Near the surface the viscous shear stress can be computed from the mean velocity measurements, so that the turbulent shear stress drop-off can be predicted. For incompressible flow of air the region of turbulent shear stress drop-off occurs extremely close to the surface, which makes actual measurements difficult. The supersonic turbulent boundary layers tend to have thicker viscous sublayers, which may help to make measurements more accessible. The sublayer becomes increasingly thicker as the Mach number

increases. In the past, hot-wire measurements of turbulent shear stress near the surface in incompressible flows produce values that are higher than expected, Sandborn, ref. 34, p. 294. The measurement difficulty was found to be due to the yawed hot wire being in a large turbulent velocity gradient, so that nonlinear averaging across the wire occurs.

The present analysis has demonstrated that an "outer region" boundary-layer similarity can be used to correlate the total shear stress distribution over the complete layer. It is also generally accepted that an "inner region" similarity may be used near the surface. For subsonic flow the velocity near the surface is found to scale as the "friction/or shear velocity," $U_\tau (\equiv \sqrt{\frac{\tau_w}{\rho_w}})$. Thus, for the region where the viscous shear stress is important, the turbulent shear stress, as well as the other turbulent stress terms, might be expected to be a universal function of the characteristic velocity, U_τ, and length, $y^* (\equiv \frac{yU_\tau}{\nu})$. Requirements for the existence of similarity for the outer region (U_τ = constant, $\partial\delta/\partial x$ = constant) are more restricted than for the inner region similarity ($\partial U_\tau/\partial x$ = constant) (see ref. 26). For super- and hypersonic flows the "inner region" similarity can be expected to become increasingly important. The extent of the viscous region increases rapidly with increasing Mach number. For a Mach number of 5 the sublayer, defined as $y^* \leq 11$, is roughly ten times larger than for the same Reynolds number at Mach number zero.

It is found that the mean velocity measurements are correlated by the inner similarity coordinates for all Mach numbers within the sublayer ($y^* < 11$). Proper inclusions of the density variation, such as that given by Van Driest, ref. 6, are found to correlate the mean velocity data out to values of y^*

greater than 200. For subsonic flow the turbulent velocity components and shear stress are found to be correlated by the inner similarity coordinates only in the viscous sublayer. Figure 6 shows a set of turbulent shear stress distributions obtained by Laufer, ref. 35, from mean velocity and pressure measurements in a fully developed pipe flow. Note that the inner region similarity for this ideal flow (U_τ = constant) only extends out to $y^* \simeq 20$. A set of hot-wire measurements of the turbulent shear stress reported by Tieleman, ref. 36, for the large Reynolds number, incompressible boundary layer is also shown on figure 6. It is difficult to obtain direct measurements of the turbulent shear stress in the wall region. The hot-wire measurements of Tieleman required up to 20% corrections due to the nonlinear effects of turbulent velocity gradients along the wire. The measurements are in agreement with the results of Laufer.

Shear stress measurements in supersonic flows do not reach into the viscous sublayer. The turbulent shear stress distributions determined from mean velocity measurements by Horstman and Owen, ref. 27, were employed to evaluate the compressible effects on the turbulent inner region similarity. These calculations were made assuming the mean flow is similar in the outer region. The insert on figure 6 shows the comparison of four sets of data taken along a cylindrical model in a Mach number 7.2 flow. For the wall coordinates used in the insert the similarity does not exist beyond $y^* \simeq 13$. The main figure 6 is a replot of the data in terms of $\frac{\tau_t}{\tau_w} \equiv \frac{\tau_t}{\rho(y)U_\tau^2}\left(\frac{\rho(y)}{\rho_w}\right)$, where $\frac{\rho(y)}{\rho_w}$ is akin to a compressible scaling parameter originally suggested by Morkovin, ref. 5. The Van Driest correction is somewhat more complex in that an integral correction for density is required. No correction is required by the y^* coordinate. The density

correction correlates the data over the region $10 < y^* < 40$, which is somewhat better than found in Laufer's pipe flow. However, due to the limited region of the inner similarity, it was not possible to compare existing compressible turbulence measurements in these coordinates. The disagreement in magnitude between the results of Horstman and Owen and incompressible results may be due to uncertainties, such as the extrapolation of the outer region similarity to the wall.

The present review demonstrates that the general magnitude of the shear stress distribution across a supersonic, adiabatic, zero pressure gradient, turbulent boundary layer can be estimated to within approximately $\pm 15\%$. The general observation of Morkovin, ref. 5, that compressible effects on the turbulence are "passive" appear valid for the shear stress distribution. It is possible that the incompressible, zero pressure gradient, shear stress distribution is an adequate model for the super- and hypersonic flows, at least up to Mach number 7.

For other than the "ideal" flat plate case information on the turbulent shear stress is quite limited. No shear stress information for highly nonadiabatic cases were found. Maise and McDonald, ref 33, demonstrated the nonsimilar nature of the mean velocity profiles for several cases, which suggest major variations may occur. A limited amount of information is available for pressure gradient boundary layers. Rose and Johnson, ref. 24, and ref. 37, have reported hot-wire and laser anemometer measurements of $\rho\overline{uv}$ for shock-wave-induced, positive pressure gradient flows. Sturek, ref. 38, gives calculations of the shear stress distributions (from evaluation of the equation of motion) for an isentropic-ramp compression flow. In subsonic flow a positive pressure gradient, which is

referred to as an adverse pressure gradient, normally produces a decrease in wall shear stress and the turbulent boundary layer approaches separation. Although, special adverse pressure gradients have been produced with constant or slightly increasing wall shear stress. For supersonic flow a positive pressure gradient can produce either (or both) boundary-layer separation and/or a "compression" of the layer with large increases in the shear stress both at the wall and in the layer. The "compression" type boundary layer decreases in thickness and developes a maximum in the total shear stress that can be many times greater than the wall value. It is difficult to conceive of a subsonic flow that is equivalent to the supersonic "compression" layer. Supersonic boundary layers experience the adverse pressure gradient effect of decreasing wall shear, which may result in flow separation, slightly upstream or in the region of a shock-wave-interaction or a compression turn. However, once through the shock wave or on an isentropic-ramp the layer is subjected to the positive pressure gradient compression effect.

Figure 7 is a plot of the turbulent shear term, $\rho\overline{uv}$, referenced to the wall shear, measured by Rose, ref. 37,* and by Rose and Johnson, ref. 24. The data of Rose is divided into three regions (figures 7a), b), and c)), the approach region, the shock wave interaction region, and the compression region. The wall shear stress increases with x-distance through the interaction and compression regions. Although the approach data for $\rho\overline{uv}$ do not agree with the expected values of the total stress, the general increase in value through and downstream of the interaction are likely to be characteristic of a "compression" layer. The laser measurements of Rose and Johnson, ref. 24, (figure 7d)) show the

*[Rose plots the term $(\rho\overline{uv} + U\overline{\rho'v})$ as the turbulent shear stress in his report.]

characteristic large increase in the total shear stress in the compression region. The pressure distribution downstream of the shock-wave interaction, reported by Rose and Johnson, is nearly constant, so the boundary layer at $x = 9.375$ should just be starting to recover to the zero pressure gradient case.

Figure 8 shows the total shear stress distributions evaluated from mean flow measurements by Sturek, ref. 38, for an isentropic-ramp -induced adverse pressure gradient flow. Although it was not clear from the paper it appears that the evaluations are not based on any similarity assumptions (some reservations were expressed on the assumption of a constant static pressure through the layer).* Both the analysis of Sturek and the measurements of Rose and Rose and Johnson indicate large increases in the magnitude of the turbulent shear stress at some distance away from the wall. The compression flow produces the increase in the wall shear stress, and also equation (12) requires that the shear stress increase away from the wall. In contrast, for incompressible, adverse pressure gradient flow a decrease in magnitude of both the wall shear stress and the maximum turbulent shear stress is normally observed. The incompressible results of Sandborn and Slogar, ref. 39, are included as an insert on figure 8 (where both profiles are referenced to the initial wall shear stress value). Thus, the supersonic "compression" flow is quite different from an incompressible, adverse pressure gradient flow. The compression effect proves to be a good "generator" of turbulent shear stress.

It is expected that a supersonic turbulent boundary layer approaching separation would have a shear stress distribution that varies much as shown in the insert

---

*The large variation of τ with distance downstream may also raise the question of the validity of the boundary-layer assumptions.

on figure 8. No turbulence data on a supersonic, separating, turbulent boundary layer was available. The actual variation from the zero pressure gradient shear stress distribution to the separation distribution obviously must occur over a very short distance.

Evaluation of the turbulent heat flux term, $q_t \equiv (-\rho\overline{vE'} - V\overline{\rho'E'} - \overline{\rho'vE'})$ (13) can be obtained in much the same manner as the shear stress term. For the insulated flat plate flow Meier and Rotta, ref. 25, have determined the turbulent heat flux from the energy equation, eq. (4). Similarity assumptions are also required for the heat flux evaluations. Figure 9(a) is a plot of the turbulent heat flux evaluated by Meier and Rotta as functions both of Mach and Reynolds number. The turbulent heat flux is found to increase with increasing Mach number, and decrease with increasing Reynolds number. (For the different Mach numbers shown, the Reynolds number ($Re \simeq 1.9 \times 10^5$) is approximately constant.

Figure 9b) shows the evaluation by Horstman and Owen, ref. 27, for the boundary layer along a cylinder with heat transfer, $T_w/T_o = 0.46$. The Reynolds number effect is also seen in the heat-transfer case (i.e., decreasing q_t with increasing Reynolds number). Positive values of q_t (not shown on figure 9b)) are obtained for the heat transfer case near the surface, however, the region near the surface is uncertain due to the similarity assumptions. Over the major portion of the boundary layer the "turbulent" Prandtl number, $Pr = \dfrac{\tau_t(\partial E/\partial y)}{q_t(\partial v/\partial y)}$, was approximately 0.9 to 0.8 for both the adiabatic and the heat-transfer case. Near the surface, where the similarity assumptions are least valid, the turbulent Prandtl number increases to values greater than one. Near the outer edge of the layers the turbulent Prandtl number drops to zero. Direct measurements of the turbulent heat flux terms have not been reported.

For the evaluation of hot-wire anemometer measurements in supersonic flow, it is usually found necessary to assume that the pressure fluctuations are zero. The assumption of zero pressure fluctuations together with the equation of state leads to the requirement that (see for example, Rose, ref. 37)

$$\overline{\rho v' E'} = -E\overline{\rho' v} \tag{14}$$

For this case the turbulent heat flux is just equal to $V\overline{\rho' E'}$. Rose, ref. 37, reports measurements of the terms $\overline{vT'}$ and $\overline{\rho' v}$, which are of experimental necessity consistent with equation (14).

The longitudinal turbulent velocity, $\sqrt{\overline{u^2}}$, has been measured by a number of experimenters. Figure 10 is a plot of the longitudinal turbulent stress, $\rho\overline{u^2}$, referenced to the local wall shear stress (square root), versus y/δ. Since the total shear stress was found to be nearly similar, when referenced to the wall shear and the boundary-layer thickness (figure 4); it might also be expected that each of the terms in the turbulent stress tensor will show an equivalent similarity in the outer region. The incompressible measurements of Zoric, ref. 26, demonstrated that all the terms in the turbulent stress tensor obtained similarity forms in the outer region. For the incompressible, high Reynolds number case evaluated by Zoric the similarity appears to hold for values of $y/\delta \geq 0.05$. The approach to similarity of the individual turbulent velocity components was found to be slower than that observed for the mean velocity or the total shear stress. The deviations of the high Reynolds number, similarity measurements of Zoric, ref. 26, and the low Reynolds number data of Klebanoff, ref. 32, in the outer region are within the experimental accuracy of the measurements.

The coordinate $\frac{\sqrt{\overline{u^2}}}{U_\tau}\sqrt{\frac{\rho(y)}{\rho_w}} \equiv \sqrt{\frac{\rho\overline{u^2}}{\tau_w}}$ was originally proposed by Morkovin, ref. 5, in 1962 totally independent of the present similarity concept. Morkovin viewed $\sqrt{\frac{\rho(y)}{\rho_w}}$ as the compressible scaling parameter. Thus, figure 10a) is equivalent to figure 3 of Morkovin's paper, except recent information has been included.

All of the supersonic measurements shown on figure 10 appear to agree closely with the incompressible measurements in the outer part of the layer. Only the data of Johnson and Rose, ref. 23 and 24, appear to agree in the region close to the surface. The fact that the hot wire and laser measurements of Johnson and Rose agree with each other was taken as justification that pressure fluctuations could be neglected in evaluating the hot-wire output. The measurements of Kistler, ref. 4, and Rose, ref. 37, in the inner part of the layer show more of an inconsistency with the data of Johnson and Rose than would be attributed to either Mach or Reynolds number variations.

The measurements of Owen and Horstman, ref. 40, and Laderman and Demetriades, ref. 17, shown on figure 10b) are for cooled wall cases of $T_w/T_{o_e} = 0.46$ and 0.38 respectively. The stabilizing effect of the cooling can act to reduce the turbulence. Thus, it is possible that the heat transfer produces the large deviations from similarity seen in figure 10b)*. Pressure fluctuations may also

---

*[Note that the total shear stress distributions evaluated by Horstman and Owen, ref. 27, and shown on figure 4, are for approximately the same flow conditions as their data of figure 10b). The shear stress profile ($R_\theta = 9.7\times10^3$) of figure 4 is at the same station, x = 225 cm, as the turbulence measurements (circles) of figure 10b). The total shear stress profiles were computed assuming similarity exists. As noted, this profile does not give the expected zero slope at the surface, so that the assumption of similarity near the surface for the hypersonic flow of Horstman and Owen appear questionable.]

be a problem in the hypersonic flows, although Laderman and Demetraides have attempted to correct for the pressure fluctuations.

Measurements of Rose, ref. 37, and Rose and Johnson, ref. 24, of the longitudinal turbulent stress variation through a shock-wave-boundary-layer interaction are shown in figure 11. The measurements in the approach region of the flows are included on figure 10a). The approach region longitudinal turbulent stress was in good agreement with the expected similarity. The effect of the shock-wave interaction, as seen from figure 11, is to increase the longitudinal turbulence in the inner two-thirds of the layer. The absolute magnitude of the longitudinal turbulent shear actually increases with x throughout the flow, since the value of τ_w increases with x. The distributions maintain a definite similarity in the outer region of the layer. Any deviation of the measurements in the outer region from the similarity profile was within the uncertainty in defining the boundary-layer thickness. The boundary-layer thickness had to be determined from temperature measurements, since the shock wave masks the velocity variation.

Figure 12 is a summary plot of reported measurements of the vertical turbulent stress, $\sqrt{\rho\overline{v^2}}$, nondimensionalized by the wall shear stress. Problems inherent in the measurement of the turbulent shear stress are also present in the measurement of $\sqrt{\overline{v^2}}$. The incompressible measurements also show larger disagreement than previously noted for the total shear stress or the longitudinal turbulent stress. The large Reynolds number boundary-layer measurements of Zoric, ref. 26, do not show the slow drop-off in $\sqrt{\overline{v^2}}$, as the wall was approached. Detailed measurements of the region very close to the surface in these large boundary layers were reported by Tieleman, ref. 36. The data of Tieleman, also included on figure 12, (note that the measurements were corrected for turbulence gradient effects on yawed wires) indicate a maximum value of $\sqrt{\overline{v^2}}$ occurs at a value of $y/\delta \simeq 0.025$,

which corresponds to a physical distance of 2.06 cm from the surface. The maximum value of $\sqrt{\overline{v^2}}$ for Klebanoff's data occurs at a value of $y/\delta \simeq 0.18$, or $y \simeq 1.37$ cm

The laser anemometer measurements of Johnson and Rose, ref. 23, for supersonic flow were found to agree reasonably well with the large Reynolds, incompressible measurements of Zoric and Tieleman, as shown on figure 12. The measurements of Rose and Johnson are perhaps slightly higher than might be expected. The agreement for both the u and v components was taken as a strong indication that the laser measurements were reasonable, although it is not established that the supersonic results should definitely agree with the incompressible data. As noted previously, these results would seem to suggest that the laser measurements of $\overline{\rho uv}$ are also valid.

Laser measurements of $\sqrt{\overline{\rho v^2}}$ downstream of a shock-wave-boundary-layer interaction were reported by Rose and Johnson, ref. 24, and are shown in figure 13. Their data show no appreciable effect due to the interaction. Hot-wire anemometry measurements through shock-wave-boundary-layer interactions are reported by Rose, ref. 37, and Rose and Johnson, ref. 24. However, it appears that questions still exist in the evaluation of hot-wire data for the measure of $\overline{v^2}$, as can be seen from figure 12.

The basic measurement with the hot-wire anemometer in compressible flow is the mass flow fluctuation, $\overline{(\rho u)'}$, since the heat transfer from the wire is equally sensitive to the density and the velocity. Thus, one would assume that the mass flow fluctuations are more accurately measured than any of the turbulent stress tensor terms. Figure 14 is a summary plot of the faired profiles of the mass flow fluctuations, referenced to the local mean mass flow, versus y/δ for

a number of supersonic and hypersonic turbulent boundary layers. The data of Kistler, ref. 4, for one particular wind tunnel shows a systematic increase in the local mass flow fluctuations with increasing Mach number. The variation of the mass flow fluctuations from one boundry layer to another is too great to suggest any systematic effects.

The mass flow fluctuations were reported by Rose, ref. 37, for the shock-wave-boundary-layer interaction. As might be expected, there was an increase in $(\overline{\rho u})'$ through the compression region. Possibly the high levels of $(\overline{\rho u})'/\bar{\rho}U$ for the approach region, shown on figure 14, may be due to the nonuniform compression effects in the upstream nozzle flow. Values of $\overline{\rho' u}$ and $\overline{\rho' w}$ are also given by Rose. The values of $\overline{\rho' w}$ were nearly zero throughout the complete flow region. The values of $\overline{\rho' v}$ are roughly one half of $\overline{\rho' u}$ in the approach region and increase to about the same values as $\overline{\rho' u}$ in the interaction and compression regions.

Temperature fluctuations have also been reported for most of the boundary layers where turbulence measurements were made. The resistance thermometer, which is an unheated hot wire, was employed for temperature measurements. In principle total temperature fluctuations can be measured directly without interaction with density, pressure, or velocity fluctuations. Unfortunately, difficulties are encountered, in that the thermometer supports may not be at the same mean temperature as the sensor. The heat-transfer error due to the supports can be large, particularly at the high Mach numbers and/or low density flows.

Figures 15a) and b) are summary plots of the reported total and static temperature fluctuations. It is not readily apparent how to correlate the

different measurements. Morkovin, ref. 5, suggested the total temperature fluctuations be nondimensionalized by dividing by the difference between free-stream static and total temperature. The present correlation employs the recovery temperature rather than the total temperature, as a possible improvement in the inclusion of hypersonic data. The hypersonic data available, Owen and Horstman, ref. 40, and Laderman and Demetriades, ref. 17, include effects of heat transfer. It is not obvious that temperature fluctuations in the presence of heat transfer would be expected to agree with those in adiabatic flow. It is surprising that the heat-transfer flows do not indicate larger temperature fluctuations than the adiabatic flows.

The static temperature fluctuation intensities are weighted by a representative mean static temperature difference across the boundary layer. This weighting is similar to that employed by Kister, ref. 4, except the recovery temperature is used (figure 15b) rather than the total temperature. These coordinates are based on the concept that the temperature fluctuation level should be proportional to the mean temperature gradient across the boundary layer, which was proposed originally by Kovasznay, ref. 2. With the exception of Rose's measurements, the supersonic boundary layers appear to be reasonably well correlated with one another. The hypersonic, heat transfer, boundary layer data agree roughly with the adiabatic static temperature variation.

Figure 16 is a summary plot of measurements of the mass flux-temperature correlation. The correlations appear to vary greatly from one boundary layer to another. The best agreement is for the cooled wall, hypersonic, boundary layers, which appear to suggest a near constant value of $R_{mT} \approx 0.6$ over most

of the layer. The supersonic data reported by Rose, ref. 41, give correlations of approximately one. Evaluation of the correlation $\overline{uT'}$, neglecting pressure fluctuations, was also reported by most of the experimenters.

The major missing measurements in compressible turbulent boundary layers are the pressure fluctuations. As noted, it was necessary to make some direct assumption regarding the magnitude of the pressure fluctuations, in order to evaluate the hot-wire measurements. Most of the evaluation techniques simply neglect the pressure fluctuations. Laderman and Demetriades, ref. 17, employed an assumption that the entropy and vorticity were out of phase, but perfectly correlated ($R_{\sigma_\tau} = -1$). Also they assumed that the sound mode was not correlated with either the entropy or vorticity modes. These assumptions, together with their data give pressure fluctuation intensities that are slightly larger than the corresponding density fluctuation intensities. In figure 10b) the measurements of $\sqrt{\frac{\overline{\rho u^2}}{\tau_w}}$ evaluated by Laderman and Demetriades, ref. 17, with the assumed corrections for pressure fluctuations are compared with measurements of Owen and Horstman, ref. 40, where the pressure fluctuations were neglected. The corrections do not appear to show a measurable effect at least in the middle region of the layer. The agreement of the hypersonic data with the incompressible, similarity profile of Zoric would appear to justify the neglect of pressure fluctuations in the outer region.

While direct measure of pressure fluctuations in the boundary layer, other than at the surface, have not proven feasible, it is possible that independent measurements of density fluctuations can be made. Recent developments in optical schlieren techniques, Wilson and Damkevala, ref. 42, and interferometry techniques, Wehrmann, ref. 43, have shown the feasibility of measuring density fluctuations.

For low density flows, Wallace, ref. 44, has used an electron beam to obtain density fluctuations. Harvey and Bushnell, ref. 45, show the variation of the density fluctuations obtained from Wallace's measurements. These measurements were taken in a hypersonic shock tunnel, with a very large temperature difference across the flow. The measured density fluctuations are much lower than would be indicated by the temperature evaluations shown on figure 15b).

Measurements of the detailed structure of the turbulent fluctuations are also available. In order to evaluate the frequency requirements of the instrumentation used for super- and hypersonic turbulence measurements, the energy spectrum is necessary. Some form of the mass flux or longitudinal turbulent velocity spectra is reported for most studies, unfortunately, it is quite difficult to compare the many different forms of the spectra that have been presented. Theoretical considerations suggest a spectra form referenced to a characteristic wave number and dissipative scale be used. For large Reynolds numbers, it is found that both atmospheric and wind tunnel turbulence spectra reduce to a universal curve for the higher wave numbers, when these scaling parameters are employed, Sandborn and Marshall, ref. 46. At the low wave number or low frequency end of the spectra the physical scale of the local flow will determine the individual spectra. The required dissipation scales are not available for the high-speed flows studied, so the evaluation of the universal spectra is not attempted. As a rough approximation, it might be assumed that the flow scales for the high speed tests are about the same. Thus, the comparison of the measured spectra in wave number coordinates might be a logical choice. Detailed measurements of the spectral variation

through a large turbulent boundary layer for incompressible flow was reported by Tieleman, ref. 36. For the incompressible flow a family of systematic developing spectra were found near the surface. (Insert, figure 17). Once the outer region, where similarity of the mean flow exists, was reached the wave number spectra are all identical and do not vary with the y-distance.

Figure 17 is a plot of the wave number spectrum;

where

$$\int_0^\infty F(k)\, dk \equiv 1 \qquad (15)$$

and

$$k = \text{wave number} = \frac{2\pi f}{U} \quad ; \text{ where } f \text{ is the frequency in hertz, and } U \text{ is the local mean velocity in ft/sec}$$

$$F(k) = \frac{U}{2\pi} \times \frac{\overline{u_f^2}}{\overline{u^2}} \quad ; \text{ where } \overline{u_f^2} \text{ is the mean square turbulent energy per unit hertz at the frequency, f, and } \overline{u^2} \text{ is the total mean square turbulent energy for all frequencies.}$$

The data of Horstman and Owen (not previously reported, but for the same flow as reported in reference 40) are for the mass flux, $(\overline{\rho u})'$. The other spectra are for the longitudinal turbulent velocity, $\overline{u^2}$. With perhaps the exception of the outer edge spectrum of Horstman and Owen (y = 3.36 cm and $y/\delta = .96$), the spectra appear to vary directly as the distance from the surface.

Figure 17 should serve as a means of determining the expected frequency range of interest in boundary-layer measurements. Once the mean velocity, as a function of y-distance, is known, the frequency corresponding to any given wave number can be computed. The lower bound on wave number might be

represented by the curve of Tieleman for $y = 17.8$ cm. The upper limit on wave number most certainly will fall within the limits of the curve given by Tieleman for $y = .0025$ cm. This curve at $y = .0025$ cm is approximately the same as the data of Morkovin, shown on figure 17, for the lower wave numbers. Note the most severe frequency requirements occur when very high velocities (thin boundary layers) are measured very close to the wall.

Spectra for temperature fluctuations are also available. The frequency content of the temperature fluctuations appear similar to the velocity fluctuations. Laderman and Demetriades, ref. 17, find that their temperature and velocity spectra are nearly the same when plotted as $\overline{u_f^2}/\overline{u^2}_{(f=o)}$ and $\overline{T_f'^2}/\overline{T'^2}_{(f=o)}$ versus $\frac{fL_x}{U}$. The scale length L_x corresponds to Taylor's macroscale of turbulence, and is slightly different for velocity and temperature. This type of scaling would not appear to correlate the measurements of either Morkovin or Horstman and Owen.

Information related to the frequency analysis of turbulent signals are also available from autocorrelation measurements. Autocorrelation measurements have been reported by Owen and Horstman, ref 47, for hypersonic boundary layers. Demetriades, ref. 48, has made similar measurements for supersonic wake flow. The autocorrelation and the energy spectra are related by a Fourier transformation. It was also demonstrated (with the exception of very close to the surface) by Owen and Horstman that the autocorrelation was approximately equal to the space-correlation for small times (.6 milliseconds) or convection distances when "Taylor's hypotheses" of space-time transformation was employed.

The scales of turbulence were originally defined by Taylor based on the space correlation coefficient, R_x,

$$\text{MACROSCALE} \qquad L_x \equiv \int_0^\infty R_x \, dx \tag{16}$$

$$\text{MACROSCALE} \qquad 1/\lambda_x^2 \equiv 2 \lim_{x \to 0} \left(\frac{1-R_x}{x^2} \right) \tag{17}$$

By use of the Fourier transformation the scales are related to the wave number spectral function, F(k) as

$$L_x = \frac{\pi}{2\overline{u^2}} F(k=o) \tag{18}$$

and

$$\frac{1}{\lambda_x^2} = \frac{1}{\overline{u^2}} \int_o^\infty k^2 \, F(k) \, dk \tag{19}$$

Owen and Horstman, ref. 40, evaluated the turbulent macroscale from their autocorrelation measurements, using equation (16) and Taylor's hypothesis. Laderman and Demetriades, ref. 17 (Philco-Ford report), employed a form of equation (18) to evaluate the macroscale in their boundary layer. Figure 18 is a plot of L_x/δ for these two hypersonic boundary layers. In figure 18a) the data of Owen and Horstman are for mass flux, while that of Laderman and Demetriades are for the longitudinal velocity. The hypersonic boundary layer scales are much larger, compared to the boundary layer thickness, than those reported for incompressible flow. Values of $(L_x/\delta) \simeq 0.25$ over the outer portion of the boundary layer were reported by Sandborn and Slogar, ref. 49, for

an incompressible boundary layer of $\delta \simeq 5$ cm. The large boundary layers of Tieleman give values of $(L_x/\delta) \simeq 0.1$. Thus, the boundary layer thickness is not an adequate scaling length for the turbulent scales.

The temperature scales measured by Owen and Horstman are smaller than the mass flux scales. For Laderman and Demetriades' measurements the scales are approximately the same.

Evaluation of the microscale from equation (19) does not appear to have been reported for supersonic flows. Owen and Horstman, ref. 40, report values obtained by curve fitting a parabola to the autocorrelation curves. The values of λ_x obtained by the evaluation were nearly equal in magnitude to the macroscale values. From subsonic measurements the ratio λ_x/L_x is found to be approximately 0.1 to 0.2. It is suspected that the frequency resolution was not adequate to define the parabola at the $t = 0$ intercept of the autocorrelation curve for Owen and Horstman's data.

The recent study of Owen and Horstman, ref. 40, includes data on the amplitude distribution of the mass flux and temperature fluctuations. Detailed measurements of the probability distributions of these fluctuations throughout the hypersonic boundary layer are presented. The mass flux fluctuation amplitude was found to be skewed negative near the surface, which was associated with large intermittent positive "spikes" in the mass flux. At the outer edge of the boundary layer the reverse effect was found. The total temperature was also found to be skewed negative near the surface. Direct measurements of the "skewness factor" $(\overline{e^3}/(\overline{e^2})^{3/2})$ are reported by Owen and Horstman.

The intermittent aspects of hypersonic boundary layers have been measured by both Owen and Horstman, ref. 40, and Laderman and Demetriades, ref. 17.

Figure 19 shows the measured values obtained for the intermittency factor, γ (where 1 is fully turbulent and 0 indicates no turbulence), across the boundary layer. The intermittency factors given by Owen and Horstman was for the mass flow fluctuations, while those of Laderman and Demetriades also include temperature fluctuations. Temperature intermittency factors reported by Owen and Horstman were slightly higher than their mass flux values. Note also that the values obtained by Owen and Horstman were determined from measurements of the "flatness factor," $\overline{e^4}/(\overline{e^2})^2$, while those of Laderman and Demetriades were found directly with a special electronic circuit.

In Figure 19 it is seen that the intermittent outer region of the hypersonic boundary layers extend over less than 20% of the boundary-layer thickness, while intermittency in the subsonic boundary layer occurs over 50 to 60% of the layer. Both compressibility and the presence of thicker sublayers in the hypersonic flow may act to reduce the intermittent region of the outer flow. Reynolds number is not expected to have a direct effect, as the large scale boundary layers of Zoric, ref. 26, and Tieleman, ref. 36, (intermittency measurements were made, but not reported) have intermittency factors much the same as measured by Klebanoff, ref. 32. Further measurements of the intermittency in both supersonic and high subsonic flows would be desired in order to determine the effect of compressibility. The early measurements of "flatness factor ratio" reported by Sandborn and Wisniewski, ref. 13, for a M = 3 boundary layer were not adequate to define the intermittency factor directly (due to inadequate electronic multiplier response); however, it appears that the extent of the intermittent outer edge was quite similar to the hypersonic measurements shown on figure 19.

The supersonic and hypersonic boundary layers also contain "intermittent" regions near the surface. The surface intermittent region is not readily observed in the subsonic boundary layers. The existence of larger sublayers in supersonic flows, no doubt, is responsible for the observed intermittency. The intermittency near the surface is also directly related to the skewness of the fluctuations found from the probability measurements.

Space-time correlation measurements were also reported by Owen and Horstman, ref. 47, for a M = 7.2 boundary layer. Similar measurements in a Mach 3 turbulent wake were reported by Demetriades, ref. 48. "Convective velocities," calculated from the measured delay time, corresponding to the maximum correlation coefficient, were obtained from these space-time measurements. The convective velocities were found to be a function of the location in the boundary layer and of the frequency. The hypersonic convective velocity measurements appear to be similar to measurements made in the large-scale subsonic boundary layer, Cliff and Sandborn, ref. 50.* In the outer region of the boundary layer the convective velocities are normally less (zero pressure gradient flow) than the local mean velocity. For the inner region the convective velocities are found to be greater than the local mean velocity. The space-time correlations study of Owen and Horstman also give a measure of the average trajectory of the turbulent fluctuations in the boundary layer.

---

*[The overall convective velocities reported by Owen and Horstman are somewhat low due to limited frequency response of the original hot-wire instrumentation. Recent measurements with improved hot-wire frequency response give higher values for the overall convective velocity in the outer region of the flow; which are in better quantitative agreement with the subsonic results.]

d) Free Shear Flow.- Wakes and jets are two types of free shear flows of major interest. The mixing of two independent flows also may be included in the free shear flows. While a number of studies are available for these types of compressible flows, they are not as well documented as the boundary layer.

Demetriades, ref. 48, 51 and 52, has made an extensive survey of an axisymmetric wake at $M = 3$. Values of the axial velocity, density, temperature and velocity-temperature fluctuations were measured. Also auto- and space-time correlations were evaluated. Using the proper coordinate transformation the compressible results were found to be "identical with their incompressible counterparts." Measurements, or the indirect evaluation, of the turbulent shear stress for a compressible wake does not appear to be available. Evaluation of the intermittency characteristics of supersonic and hypersonic wakes were reported by Demetriades, ref. 52, and by Levensteins and Krummins, ref. 53. Estimates of turbulent scales were also reported in these papers. The wake intermittency for compressible flow was found to be nearly the same as the incompressible measurements.

A number of turbulence measurements have been reported for real gas type turbulent wakes; refs. 54 through 57. These data were for wakes behind projectiles rather than for the statistically steady flows discussed above. Autocorrelations, spectrum and time scales are obtained from these measurements. New techniques of measuring instantaneous wake profiles and turbulence are presented in references 58 and 59.

Very little information on turbulence measurements in compressible jets was found in the present survey. Estimates of turbulent effects, such as eddy-viscosity or mixing lengths, are available mainly from incompressible

measurements. The recent paper of Peters, Chriss and Paulk, ref. 60, contain evaluations of the shear stress based on mean flow measurements for subsonic jets. Measurements of the intermittency factor for a jet with an initial velocity of 693 ft/sec were reported by Maestrello and McDaid, ref. 61. These subsonic compressible measurements agree with the incompressible intermittency data.

A recent conference on "Free Turbulent Shear Flow," ref. 62, has examined in great detail existing methods of computing free shear flows. There was some evidence from the mean flow calculations that the compressible effects on turbulence may be more pronounced for the free shear flows.

CONCLUSIONS

A direct comparison of measured terms in the turbulent stress tensor for zero pressure gradient, super- and hypersonic, turbulent boundary layers with large Reynolds number, incompressible, boundary layers was found to show remarkable agreement. The turbulent stress terms were scaled with the wall shear stress and the boundary-layer thickness. While some variations in the data were found near the surface, the outer region of the zero pressure gradient, turbulent boundary layer appears to be surprisingly similar for all Mach numbers.

Mean flow evaluations of the total shear stress distributions across the whole, zero pressure gradient, turbulent, boundary layer was also found to correlate nearly independent of Mach number. The total shear stress distribution for the compressible boundary layers was in good agreement with the measured Reynolds shear stress $(\overline{\rho uv})$ term for incompressible, zero pressure gradient,

layers. Recent laser anemometer measurements, by Johnson and Rose at a Mach number of 2.9, of $\overline{\rho uv}$ are also in reasonable agreement with the expected total shear stress over the outer 60% of the boundary layer. Near the surface the laser measurements are systematically lower than the expected values. The laser measurements are only slightly higher than the individual stress components ($\rho\overline{u^2}$ and $\rho\overline{v^2}$) measured in incompressible flow. Thus, the direct laser measurements appear to be reasonable over the complete boundary layer. The disagreement between the measurement of $\overline{\rho uv}$ and the total shear stress might be taken with some reservation to suggest that the Reynolds stress term may not be the only important turbulent shear stress term in supersonic boundary layers.

The correlation of the measurements, together with the incompressible data can be proposed as a check on the super- and hypersonic measuring techniques. Figure 20 is the proposed summary plot of the expected variation of the Reynolds stress tensor terms. Adiabatic, zero pressure gradient, turbulent, supersonic, boundary layers are expected to agree with these curves over the outer 50 to 60% of the layer. Near the surface the viscous sublayer will cause deviations. The sublayer thickness will increase in size by greater than a factor of 10 as the Mach number goes from 0 to 5.

Hot-wire anemometer measurements of the longitudinal component of velocity fluctuations, neglecting pressure fluctuations, for at least supersonic Mach numbers appear to be reasonable. However, measurements of the vertical component of the turbulent velocity and the Reynolds shear stress with yawed hot wires appear questionable. Direct measurements of the longitudinal mass flow fluctuations with the hot-wire anemometer show considerable variation from

one set of data to another. The hot wire should be most sensitive to the mass flow, so it appears that use of the local mean values of the mass flow are not adequate to normalize the results. Considerable variation is also observed for the temperature fluctuation measurements.

The spectrum of mass flow fluctuation for super- and hypersonic flows were also found to agree with incompressible results when compared on a wave number plot. The resultant spectra should serve as a direct approximation of the frequency content of a given boundary-layer measurement.

Measurements of the intermittency of the outer region of super- and hypersonic boundary layers shows a marked difference from the incompressible layer. The intermittency extends over a much smaller percentage of the layer ($\sim$ 20%) for the high-speed flows, compared to the incompressible flow ($\sim$ 50%)

Evaluation of mass-flow fluctuation intensity in the free stream of super- and hypersonic wind tunnels indicate the intensity increases approximately as Mach number squared. The level is found to decrease with Reynolds number, and also would be expected to decrease with increasing tunnel size. The size effect is not evident in the hypersonic tunnels. For Mach numbers greater than 2.5 the mass flow fluctuations should not be influenced by the inlet conditions.

REFERENCES

1. Kovasznay, L. S. G.: The Hot Wire Anemometer in Supersonic Flow. Journal of the Aeronautical Sciences, vol. 17, pp. 565-572, 1950.

2. Kovasznay, L. S. G.: Turbulence in Supersonic Flow. Journal of the Aeronautical Sciences, vol. 20, no. 10, p. 657, 1953.

3. Morkovin, M. V., and Phinney, R. E.: Extended Applications of Hot Wire Anemometry to High-Speed Turbulent Boundary Layers. AFDSR TN-58-469, Johns Hopkins Univ., Dept of Aeronautics, 1958.

4. Kistler, A. L.: Fluctuation Measurements in a Supersonic Turbulent Boundary Layer. Physics of Fluids, vol. 2, p. 290, 1959.

5. Morkovin, M. V.: Effects of Compressibility on Turbulent Flows. International Symposium on the "Mecanique de la Turbulence," Centre National de la Recherche Scientifique, Paris, p. 367-380, 1962.

6. Van Driest, F. R.: Turbulent Boundary Layer in Compressible Fluids. Jour. Aeronautical Sciences, vol. 18, no. 3, p. 145-160, 1951.

7. Schubauer, G. B., and Tchen, C. M: Turbulent Flow. Princeton Aeronautical Paperbacks. C. D. Donaldson, ed., Princeton University Press, 1961.

8. Rotta, J. C.: Turbulent Boundary Layers in Incompressible Flow. Progress in the Aeronautical Sciences, vol. 2, Boundary Layer Problems. Ed. by A. Ferri, et. al., The MacMillan Co., New York, 1962.

9. Ross, A. O.: Determination of Boundary Layer Transition Reynolds Number by Surface-Temperature Measurement of a 10° Cone in Various NACA Supersonic Wind Tunnels. NACA TN 3020, 1953

10. Fischer, M. C., and Wagner, R. D: Transition and Hot-Wire Measurements in Hypersonic Helium Flow. AIAA Jour., vol. 10, No. 10, p. 1326, 1972.

11. Stainback, P. C., Wagner, R. D., Owen F. K. and Horstman, C. C.: Experimental Studies of Hypersonic Boundary Layer Transition and the Effects of Wind Tunnel Disturbances. NASA TN D-7453, 1973.

12. Pate, S. R., and Schueler, C. J.: Radiated Aerodynamic Noise Effects on Boundary Layer Transition in Supersonic and Hypersonic Wind Tunnels. AIAA Jour., vol 7, no. 3, p. 450, 1969.

13. Sandborn, V. A., and Wisniewski, R. J.: Hot Wire Exploration of Transition on Cones in Supersonic Flow. Proceedings of the 1960 Heat Transfer and Fluid Mechanics Institute, Stanford Univ. Press, 1960.

14. Laufer, J.: Factors Affecting Transition Reynolds Numbers of Models in Supersonic Wind Tunnels. Jour. Aeronautical Sciences, vol. 21, no. 7, p. 497, 1954.

15. Morkovin, M. V.: On Supersonic Wind Tunnels with Low Free-Stream Disturbances. Air Force Office of Scientific Research, TN 56-540, 1956.

16. Laufer, J.: Aerodynamic Noise in Supersonic Wind Tunnels, Jour. Aeronautical Sciences, vol. 28, p. 685, 1961.

17. Laderman, A. J., and Demetriades, A.: Measurements of the Mean and Turbulent Flow in a Cooled-Wall Boundary Layer at Mach 9.37. AIAA paper 72-73, San Diego, Calif., 1972. See also Philco-Ford Pub. No. V-5079, 1972.

18. Donaldson, J. C., and Wallace, J. P.: Flow Fluctuation Measurements at Mach Number 4 in the Test Section of the 12-Inch Supersonic Tunnel. Arnold Engineering Development Center, AEDC-TR-71-143, 1969.

19. Kjellström, B., and Hedberg. S: Calibration Experiments with a DISA Hot-Wire Anemometer. Aktiebolaget ATomenergi Rep. AE 388, 1968.

20. Durst, F., Launder, B. E., and Kjellström, B: The Effect of Compressibility on the Shear-Stress Distribution in Turbulent Pipe Flow. Aeronautical Jour. Roy. Aero. Soc., vol 75, p. 55-57, 1971.

21. Gibbings, J. C., and Mikulla, V.: Measurements of Reynolds Stresses in Compressible Flow. Univ. of Liverpool, ARC Rep. 34540, FM 4408, 1973.

22. Serafini, J. S.: Wall-Pressure Fluctuations and Pressure-Velocity Correlations in a Turbulent Boundary Layer. NASA TR R-165, 1963.

23. Johnson, D. A., and Rose, W. C.: Measurements of Turbulent Transport Properties in a Supersonic Boundary Layer Flow Using Laser Velocimeter and Hot Wire Anemometer Techniques. AIAA Paper No. 73-1045, Oct. 1973.

24. Rose, W. C., and Johnson, D. A.: A Study of Shock-Wave Turbulent Boundary Layer Interaction Using Laser Velocimeter and Hot-Wire Anemometer Techniques. AIAA Paper 74-95 , Jan. 1974.

25. Meier, H. V., and Rotta, J. C.: Experimental and Theoretical Investigations of Temperature Distributions in Supersonic Boundary Layers. AIAA Paper 70-744, Los Angeles, Calif., 1970.

26. Zoric, D. L.: Approach of Turbulent Boundary Layer to Similarity. Ph.D Dissertation, Colorado State Univ. (Report CER 68-69DLZ9) 1968.

27. Horstman, C. C., and Owen, F. K.: Turbulent Properties of a Compressible Boundary Layer. AIAA Jour., vol. 10, no. 11, p. 1418-1424, 1972. (Shear stress profile for $R_\theta = 9.7 \times 10^3$ is an updated one obtained since the paper was published.)

28. Danberg, J. E.: Characteristics of the Turbulent Boundary Layer with Heat and Mass Transfer: Data Tabulation. NOLTR 67-6, U.S. Navy, 1967.

29. Bushnell, D. M., and Morris, D. J.: Shear-Stress, Eddy-Viscosity, and Mixing-Length Distributions in Hypersonic Turbulent Boundary Layers. NASA TM X-2310, 1971.

30. Samuels, R. D., Peterson, J. B., and Adcock, J. B.: Experimental Investigation of the Turbulent Boundary Layer at a Mach Number of 6 with Heat Transfer at High Reynolds Number. NASA TN D-3858, 1967.

31. Rochelle, W. C.: Prandtl Number Distribution in a Turbulent Boundary Layer with Heat Transfer at Supersonic Speeds. Defense Research Lab., Univ. of Texas, Rept. No. 508 (AD-427156), 1963.

32. Klebanoff, P. S.: Characteristics of Turbulence in a Boundary Layer with Zero Pressure Gradient. NACA Tech. Rept. 1247, 1955.

33. Maise, G., and McDonald, H.: Mixing Length and Kinematic Eddy Viscosity in a Compressible Boundary Layer. AIAA Jour., vol. 6, no. 1, p. 73-80, 1968.

34. Sandborn, V. A.: Resistance Temperature Transducers. Metrology Press, Fort Collins, Colo., 1972.

35. Laufer, J.: The Structure of Turbulence in Fully Developed Pipe Flow. NACA Tech. Rept. No. 1174, 1954.

36. Tieleman, H. W.: Viscous Region of Turbulent Boundary Layer. Ph.D. Dissertation, Colorado State University, Report No. CER67-68HWT21, 1967.

37. Rose, W. C.: The Behaivor of a Compressible Turbulent Boundary Layer in a Shock-Wave-Induced Adverse Pressure Gradient. NASA TN D-7092, 1973.

38. Sturek, W. B.: Calculations of Turbulent Shear Stress in Supersonic Turbulent Boundary Layer Zero and Adverse Pressure Gradient Flow. AIAA Paper No. 73-166, Washington, D. C., 1973.

39. Sandborn, V. A. and Slogar, R. J.: Study of the Momentum Distribution of Turbulent Boundary Layers in Adverse Pressure Gradients. NACA TN 3264, 1955.

40. Owen, F. K., and Horstman, C. C.: Turbulent Measurements in an Equilibrium Hypersonic Boundary Layer, AIAA Paper 74-93 , Jan. 1974.

41. Rose, W. C.: Turbulence Measurements in a Compressible Boundary Layer Subjected to a Shock-Wave-Induced Adverse Pressure Gradient. AIAA Paper No. 73-167, Washington, D. C., 1973.

42. Wilson, L. N., and Damkevala, R. J.: Statistical Properties of Turbulent Density Fluctuations. Jour. Fluid Mechanics, vol. 43, pt. 2, pp. 291-303, 1970.

43. Wehrmann, O. H.: Velocity and Density Measurements in a Free Jet. AGARD Conf. Proceedings No. 93, Turbulent Shear Flow, AGARD-CP-93, 1971.

44. Wallace, J. E.: Hypersonic Turbulent Boundary-Layer Measurements Using an Electron Beam. AIAA Jour., vol. 7, no. 4, p. 757, 1969.

45. Harvey, W. D., and Bushnell, D. M.: Velocity Fluctuation Intensities in a Hypersonic Turbulent Boundary Layer. AIAA Jour., vol. 7, no. 4, p. 760, 1969.

46. Sandborn, V. A., and Marshall, R. D.: Local Isotropy in Wind Tunnel Turbulence. Colorado State University Report CER65 VAS-RDM 71, 1965.

47. Owen, F. K., and Horstman, C. C.: On the Structure of Hypersonic Turbulent Boundary Layers. Jour. Fluid Mechanics, vol. 53, pt. 4, pp. 611-636, 1972.

48. Demetriades, A.: Theory of Hot-Wire Correlation Measurements in Compressible Flow with Application to Wakes. AIAA Paper No. 72-117, San Diego, Calif., 1972.

49. Sandborn, V. A., and Slogar, R. J.: Longitudinal Turbulent Spectrum Survey of Boundary Layers in Adverse Pressure Gradients. NACA TN 3453, 1955.

50. Cliff, W. C., and Sandborn, V. A.: Measurements and a Model for Convective Velocities in the Turbulent Boundary Layer. NASA TN D-7416, 1973.

51. Demetriades, A.: Turbulent Measurements in an Axisymmetric Compressible Wake. Physics of Fluids, Vol. 11, no. 9, p. 1841, 1968.

52. Demetriades, A.: Turbulent Front Structure of an Axisymmetric Compressible Wake. Jour. of Fluid Mechanics, vol. 34, pt. 3, p. 465, 1968.

53. Levensteins, Z. J., and Krumins, M. V.: Aerodynamic Characteristics of Hypersonic Wakes. AIAA Jour., vol. 5, no. 9, p. 1596, 1967.

54. Fox, J., Webb, W. H., Jones, B. G., and Hammitt, A. G.: Hot-Wire Measurements of Wake Turbulence in a Ballistic Range. AIAA Jour., Vol. 5, No. 1, p. 99, 1967.

55. Eckerman, J., and Lien, H.: Interferometric Analysis of Density Fluctuations in Hypersonic Turbulent Wakes. AIAA Paper 65-809, 1965.

56. Clay, W. G., Herrmann, J., and Slattery, R. E.: Statistical Properties of the Turbulent Wake Behind Hypersonic Spheres. Physics of Fluids, vol. 8, p. 1792, 1965.

57. Fox, J., and Rungaldier, H.: Electron Density Fluctuations Measurements in Projectile Wakes. AIAA Paper No. 70-730, San Diego, Calif., 1970.

58. Dionne, J. G. G., Heckman, D., Lahaye, C., Sévigny, L., and Tardif, L.: Fluid Dynamic Properties of Turbulent Wakes of Hypersonic Spheres. Proceedings on Turbulent Shear Flow. AGARD-CP-93, p. 13-1, 1971.

59. Schneiderman, A. M.: Measurements of the Instantaneous Spatial Distribution of a Passive Scalar in an Axisymmetric Turbulent Wake. Proceedings on Turbulent Shear Flow. AGARD-CP-93, p. 14-1, 1971.

60. Peters, C. E., Chriss, D. E., and Paulk, R. A.: Turbulent Transport Properties in Subsonic Coaxial Free Mixing Systems. AIAA Paper No. 69-681, San Francisco, Calif., 1969.

61. Maestrello, L., and McDaid, E.: Acoustic Characteristics of a High-Subsonic Jet. AIAA Jour., vol. 9, no. 6, p. 1058, 1971.

62. Free Turbulent Shear Flow, volume I - Conference Proceedings, NASA SP-321, 1972.

63. Laderman, A. J.: Effect of Mass Addition and Angle-of-Attack on the Hypersonic Boundary Layer Turbulence Over a Slender Cone. Philco-Ford Corp. Pub. No. U-6047, 1973.

64. Wise, B., and Schultz, D. L.: Trubulence Measurements in Supersonic Flow With the Hot Wire Anemometer. ARC-Cp366, Tech Rep. 18,373, Oxford University, Rept. No. 83, 1957.

65. Demtriades, A., and Laderman, A. J.: Reynolds Stress Measurements in a Hypersonic Boundary Layer. AIAA Jour., vol. 11, No. 11, p. 1594, 1973.

66. Lee, R. E., Yanta, W. J., and Leonas, A. C.: Velocity Profile, Skin-Friction Balance and Heat Transfer Measurements of the Turbulent Boundary Layer at Mach 5 and Zero-Pressure Gradient. NOLTR 69-106, U. S. Navy, June 16, 1969.

67. Adcock, J. B., Peterson, J. B., and McRee, D. I: Experimental Investigation of a Turbulent Boundary Layer at Mach 6, High Reynolds Number and Zero Heat Transfer. NASA TN D-2907, 1965.

68. Perry, J. H.: An Experimental Study of the Turbulent Hypersonic Boundary Layer at High Rates of Wall Heat Transfer. Ph.D. Thesis, Univ. of Southampton, June 1968.

69. Fiore, A. W.: Turbulent Boundary Layer Measurements at Hypersonic Mach Numbers. ARL 70-0166, U. S. Air Force, Aug. 1970.

70. Fischer, M. C., Maddalon, D. V., Weinstein, L. M., and Wagner, R. D.: Boundary-Layer Surveys on a Nozzle Wall at $M_\infty \simeq 20$ Including Hot-Wire Fluctuation Measurements. AIAA Paper No. 70-746, June-July 1970.

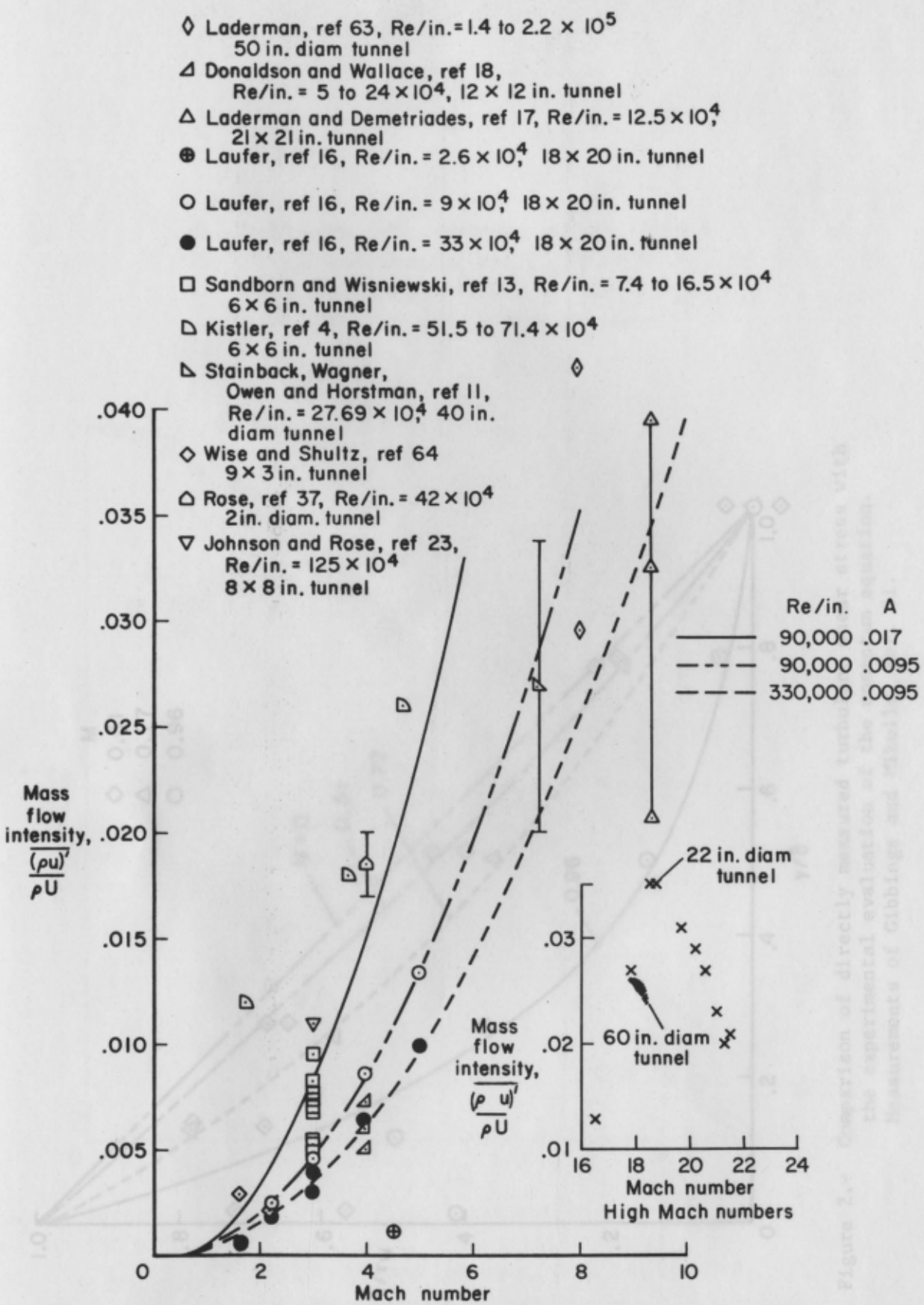

Figure 1.- Measured free-stream mass flow fluctuations. Curves are for the relation $\frac{\overline{(\rho u)'}}{\rho v} = A Re/in^{-.25}(M^2 - .5)$

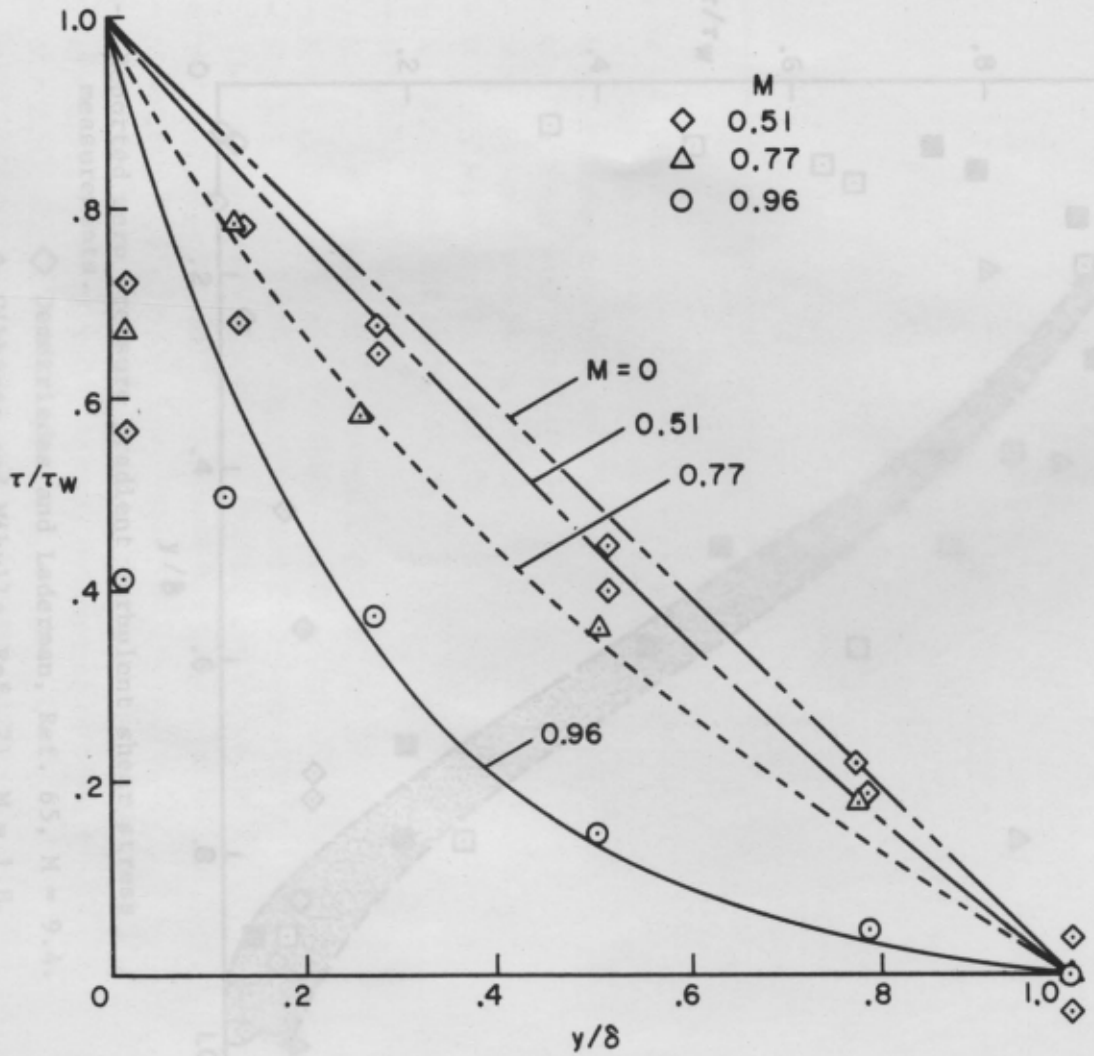

Figure 2.- Comparison of directly measured turbulent shear stress with the experimental evaluation of the momentum equation. Measurements of Gibbings and Mikulla, Ref. 21.

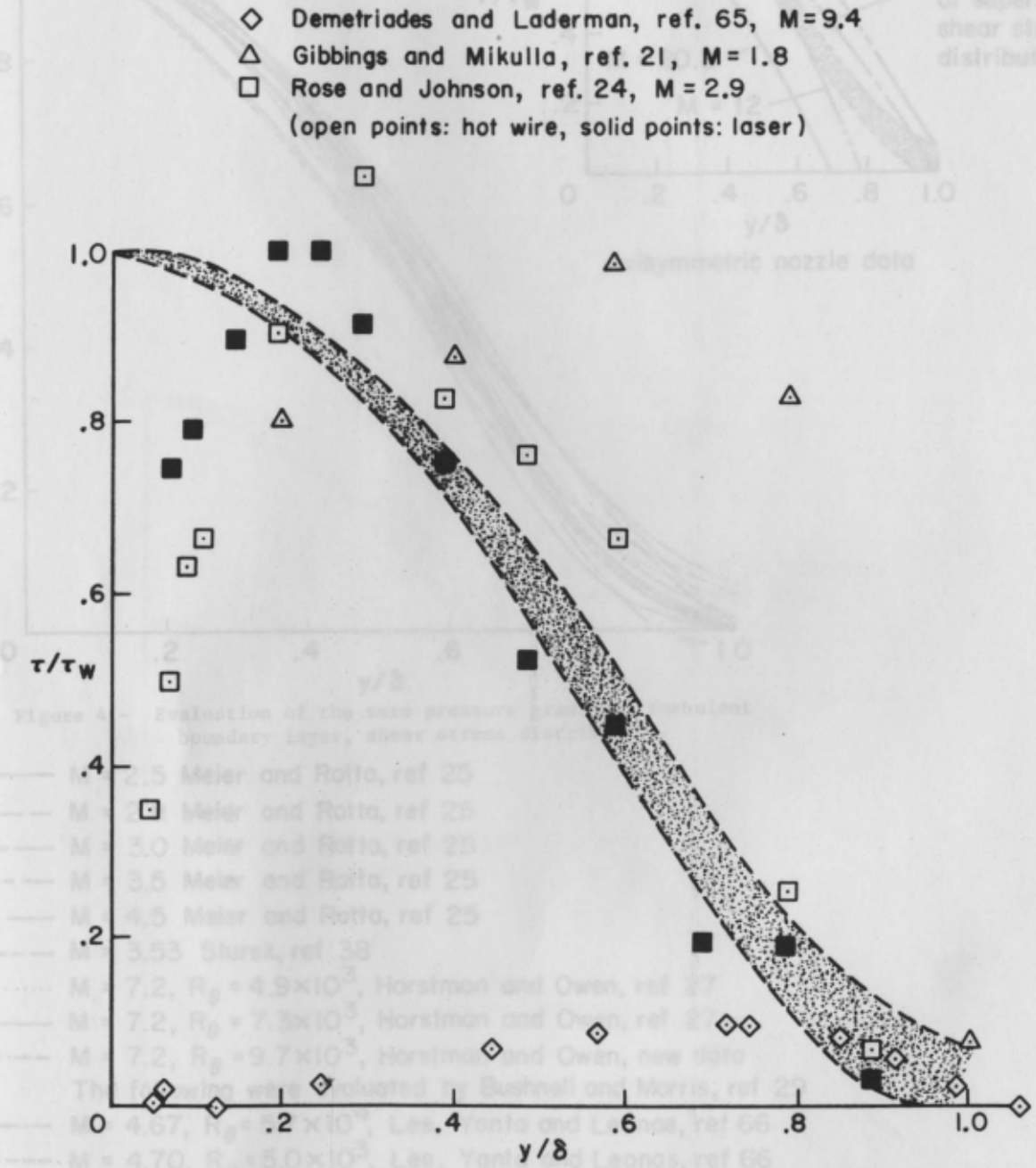

Figure 3.- Reported zero pressure gradient turbulent shear stress measurements.

◇ Demetriades and Laderman, Ref. 65, M = 9.4.

△ Gibbings and Mikulla, Ref. 21, M = 1.8.

□ Rose and Johnson, M = 2.9 (open points; hot wire, solid: laser) Ref. 24.

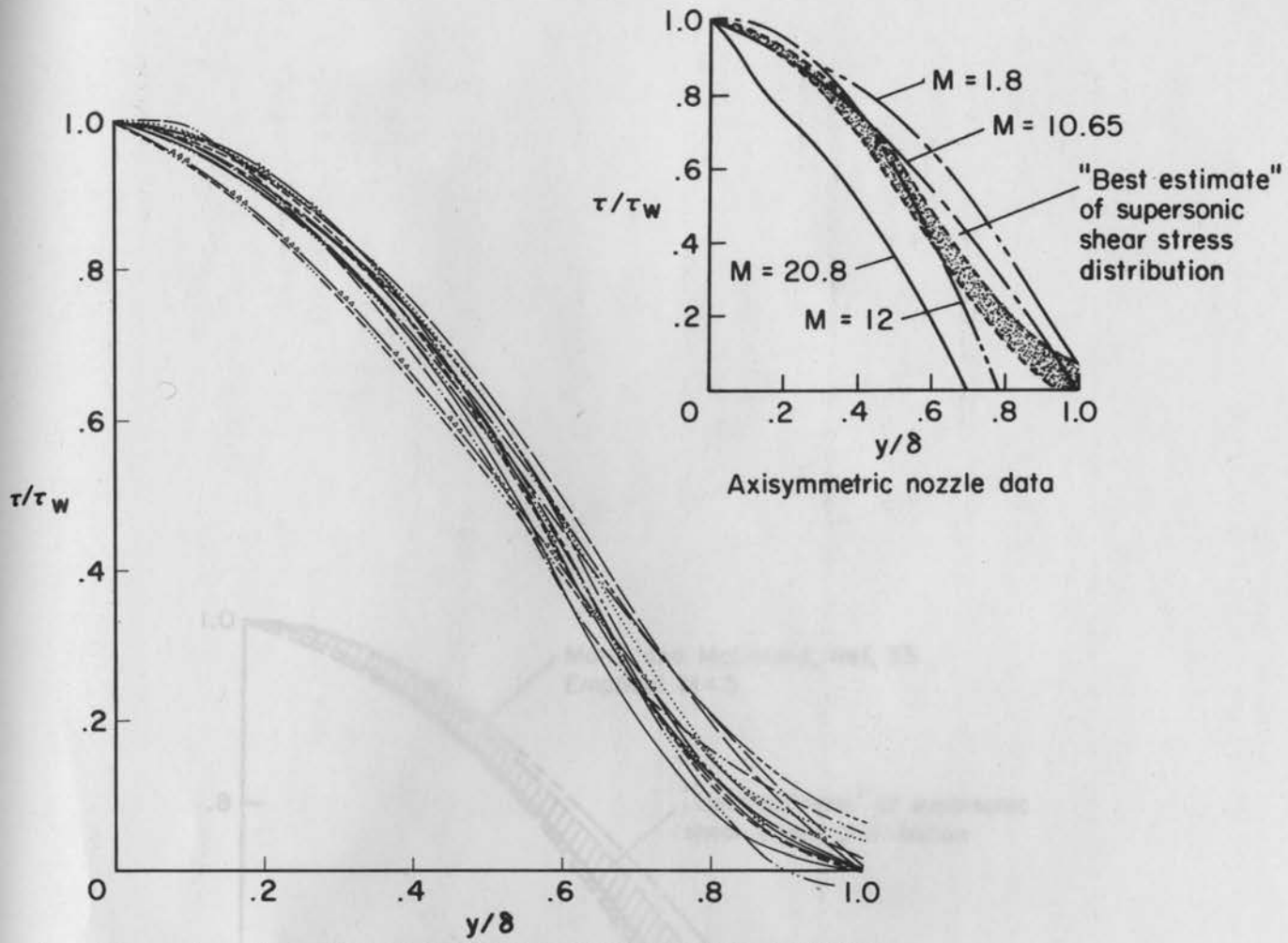

Figure 4.- Evaluation of the zero pressure gradient, turbulent boundary layer, shear stress distribution.

——— M = 2.5 Meier and Rotta, ref 25
— — — M = 2.8 Meier and Rotta, ref 25
— - — M = 3.0 Meier and Rotta, ref 25
— - - — M = 3.5 Meier and Rotta, ref 25
— — M = 4.5 Meier and Rotta, ref 25
— - - - — M = 3.53 Sturek, ref 38
..... M = 7.2, $R_\theta = 4.9 \times 10^3$, Horstman and Owen, ref 27
.....— M = 7.2, $R_\theta = 7.3 \times 10^3$, Horstman and Owen, ref 27
·-·-·-·— M = 7.2, $R_\theta = 9.7 \times 10^3$, Horstman and Owen, new data

The following were evaluated by Bushnell and Morris, ref 29

—·—·— M = 4.67, $R_\theta = 5.7 \times 10^4$, Lee, Yanta and Leonas, ref 66
····— - - - M = 4.70, $R_\theta = 5.0 \times 10^3$, Lee, Yanta and Leonas, ref 66
—··— M = 5.98, $R_\theta = 1.28 \times 10^4$, Samuels, Peterson and Adcock, ref 30
—ww— M = 6.02, $R_\theta = 1.40 \times 10^4$, Adcock, Peterson and McRee, ref 67
—ΔΔΔ— M = 6.50, $R_\theta = 2.53 \times 10^3$, Damberg, ref 28

High Mach number data evaluated by Bushnell and Morris, ref 29

M = 10.65 Perry, ref 68
M = 12 Fiore, ref 69
M = 20.8 Fisher, Maddalon, Weinstein and Wagner, ref 70
M = 1.8 Gibbings and Mikulla, ref 21

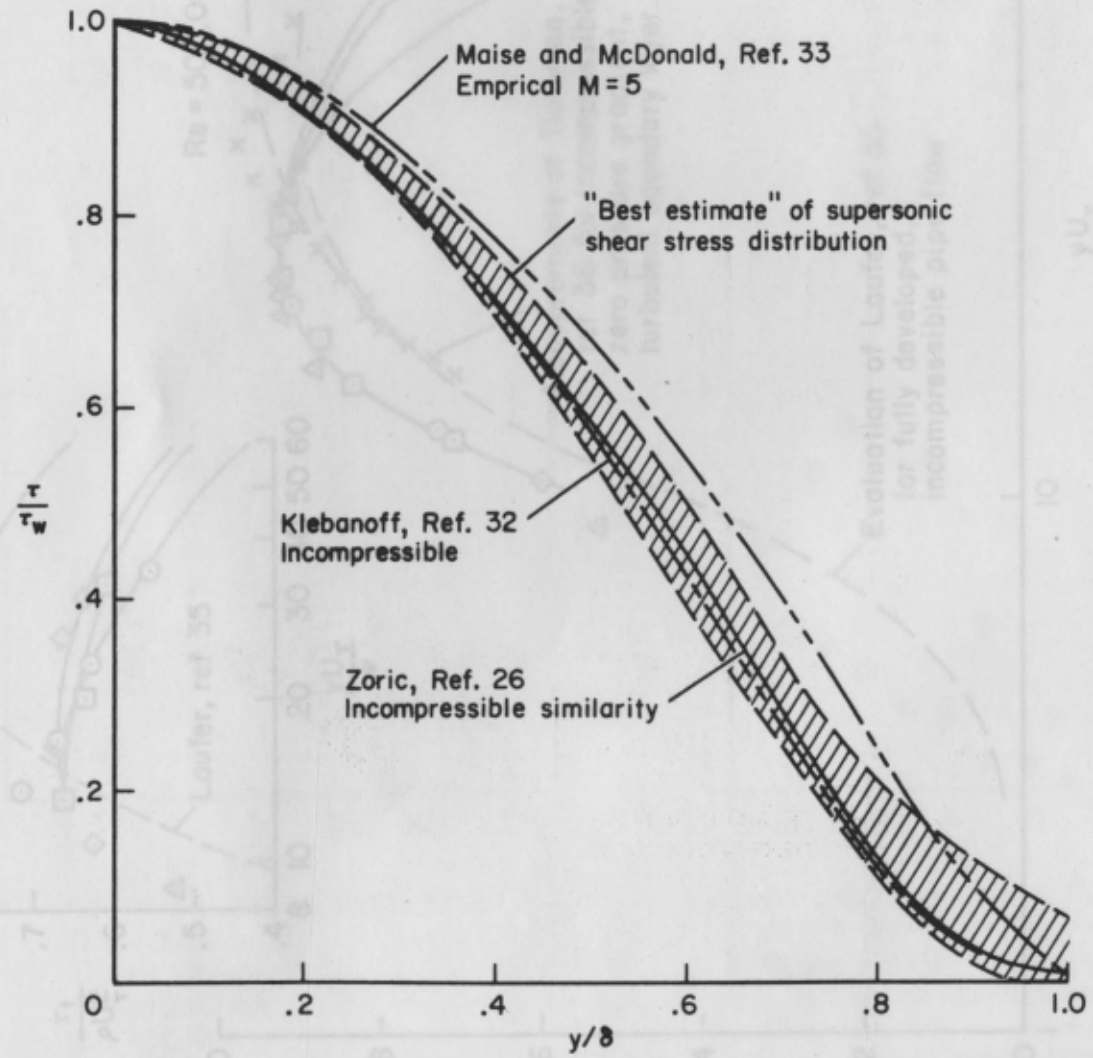

Figure 5.— Comparison of estimated supersonic shear stress with incompressible measurements and the empirical prediction of Maise and McDonald.

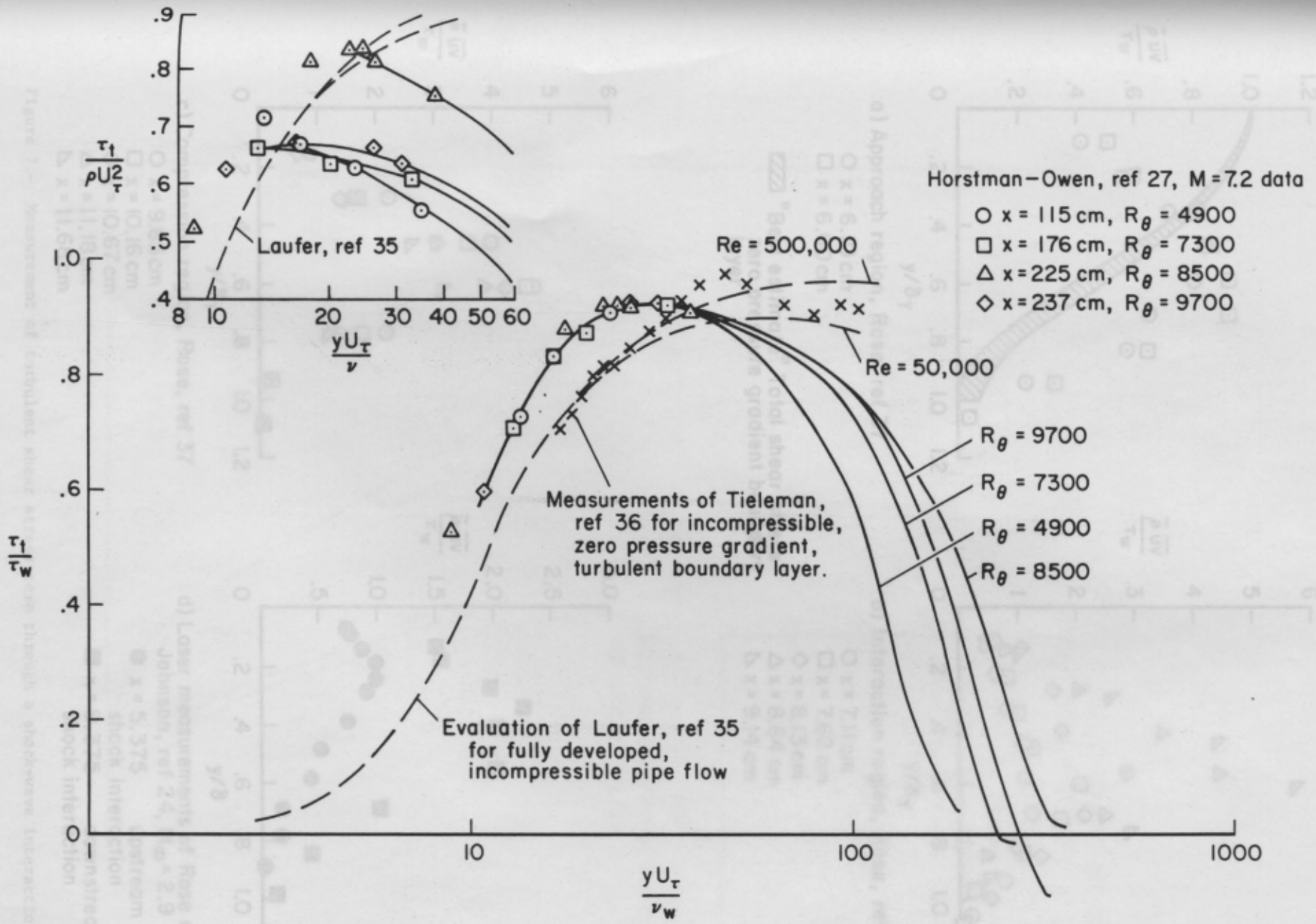

Figure 6.- Inner region similarity plot of the turbulent shear stress for the data evaluated by Horstman and Owen, Ref. 20.

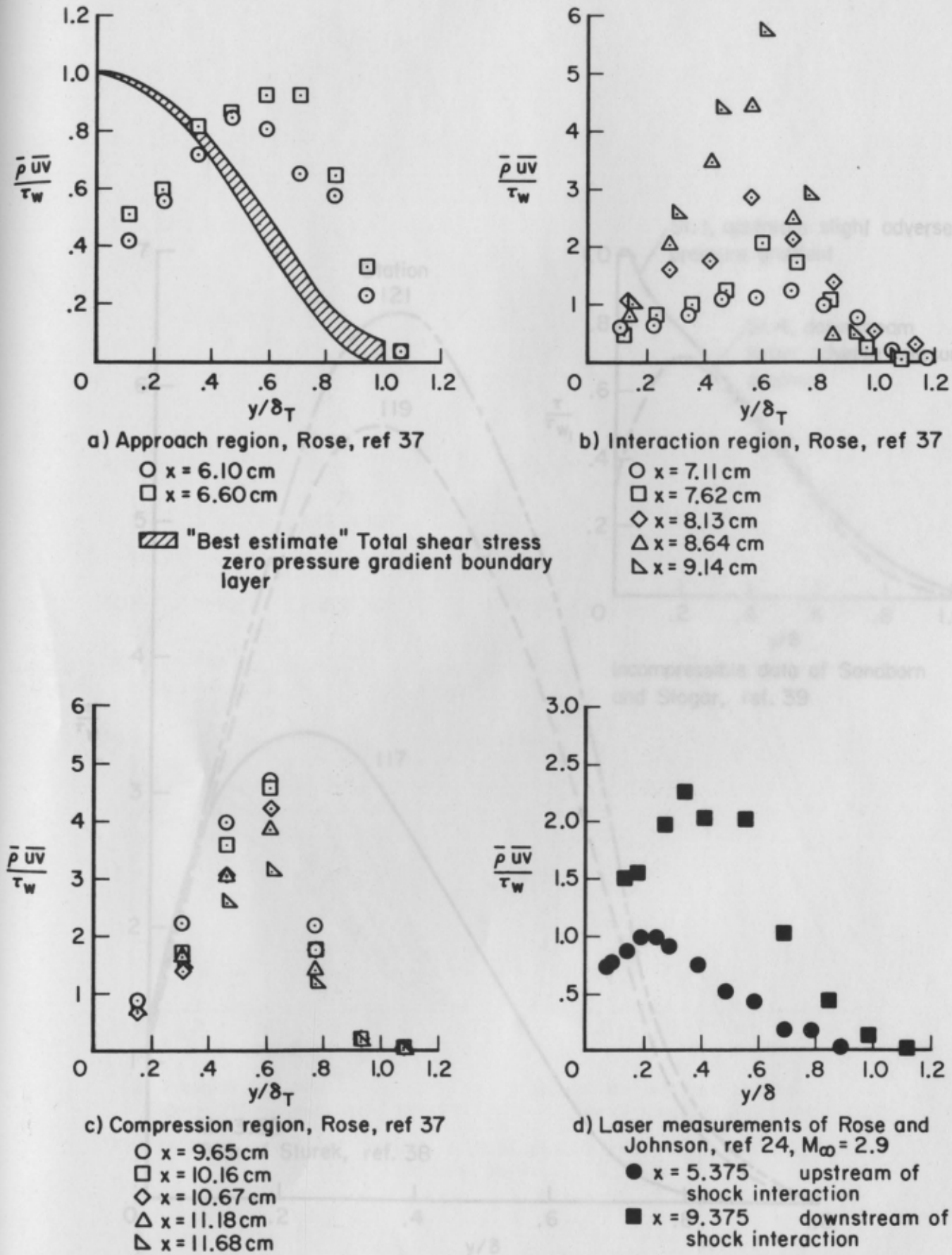

Figure 7.- Measurement of turbulent shear stress term through a shock-wave interaction.

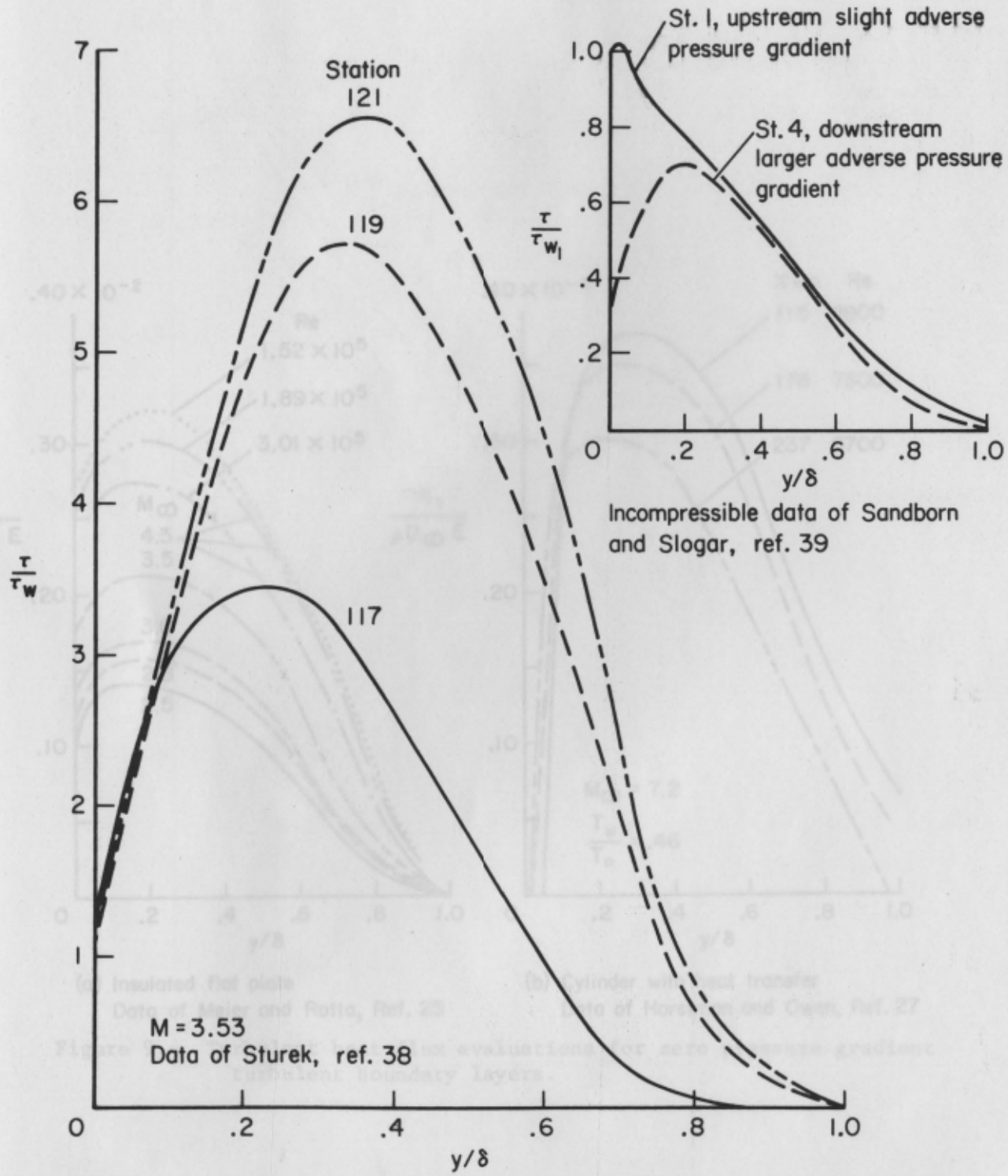

Figure 8.- Adverse pressure gradient shear stress distributions.

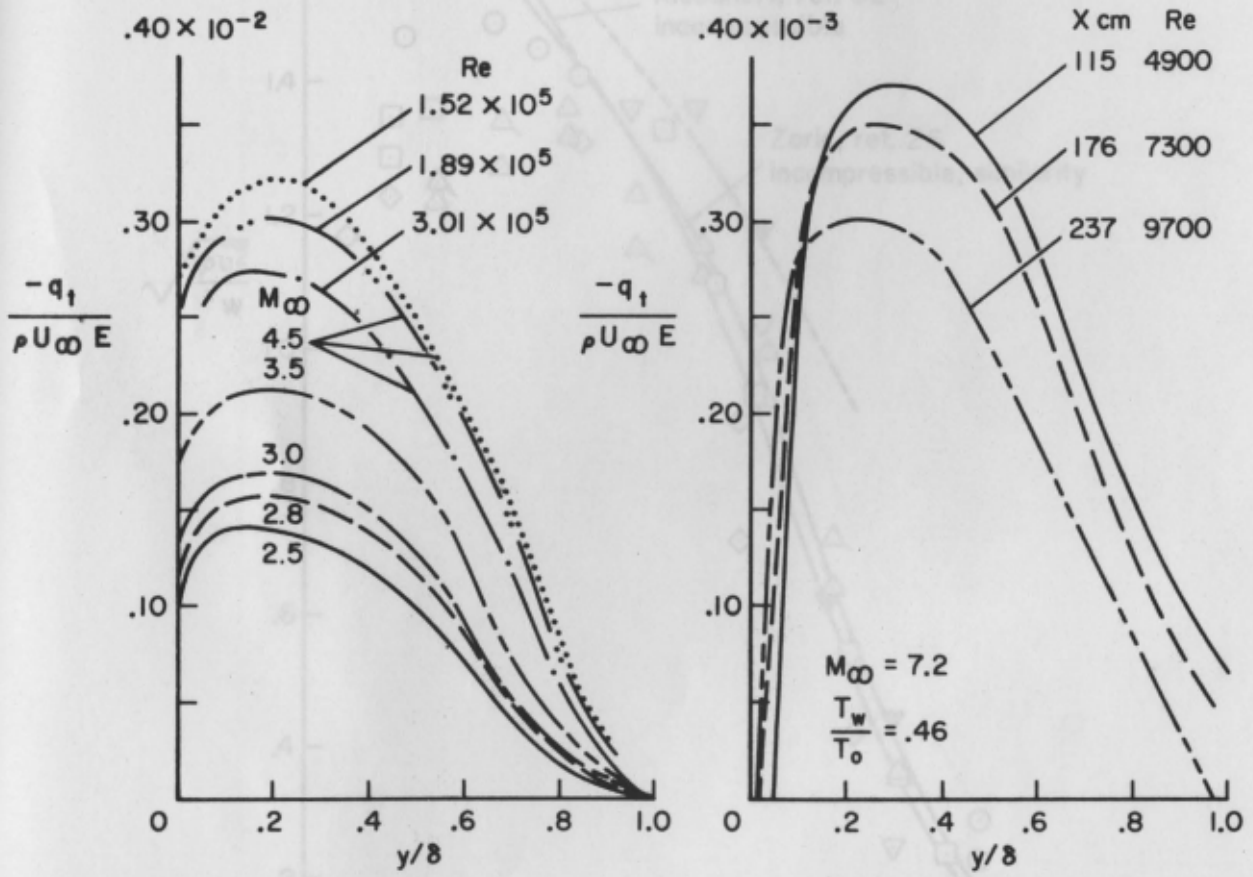

(a) Insulated flat plate
Data of Meier and Rotta, Ref. 25

(b) Cylinder with heat transfer
Data of Horstman and Owen, Ref. 27

Figure 9.- Turbulent heat flux evaluations for zero pressure gradient turbulent boundary layers.

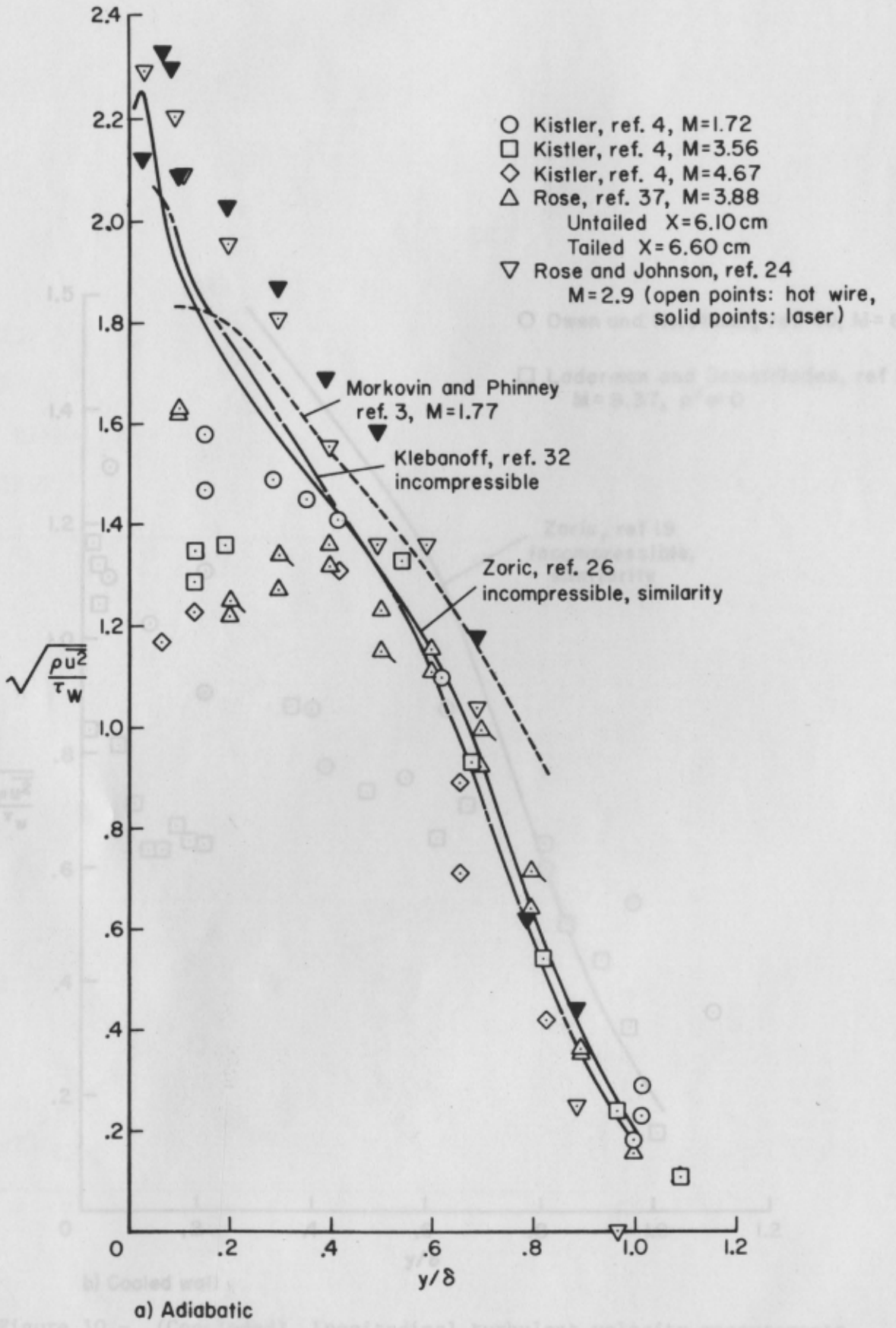

Figure 10.- Longitudinal turbulent velocity measurements in zero pressure gradient boundary layers.

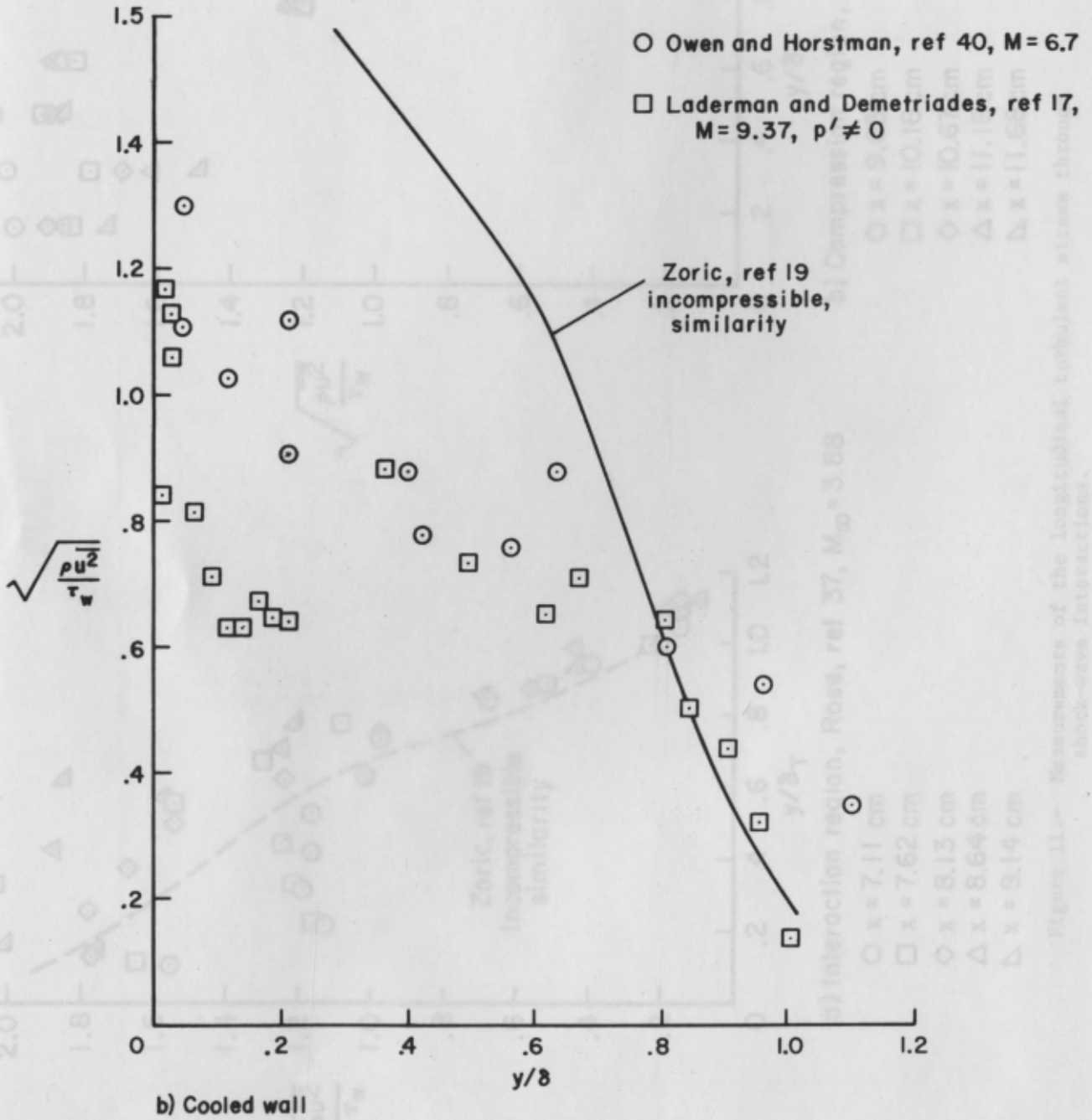

Figure 10.- (Concluded) Longitudinal turbulent velocity measurements in zero pressure gradient boundary layers.

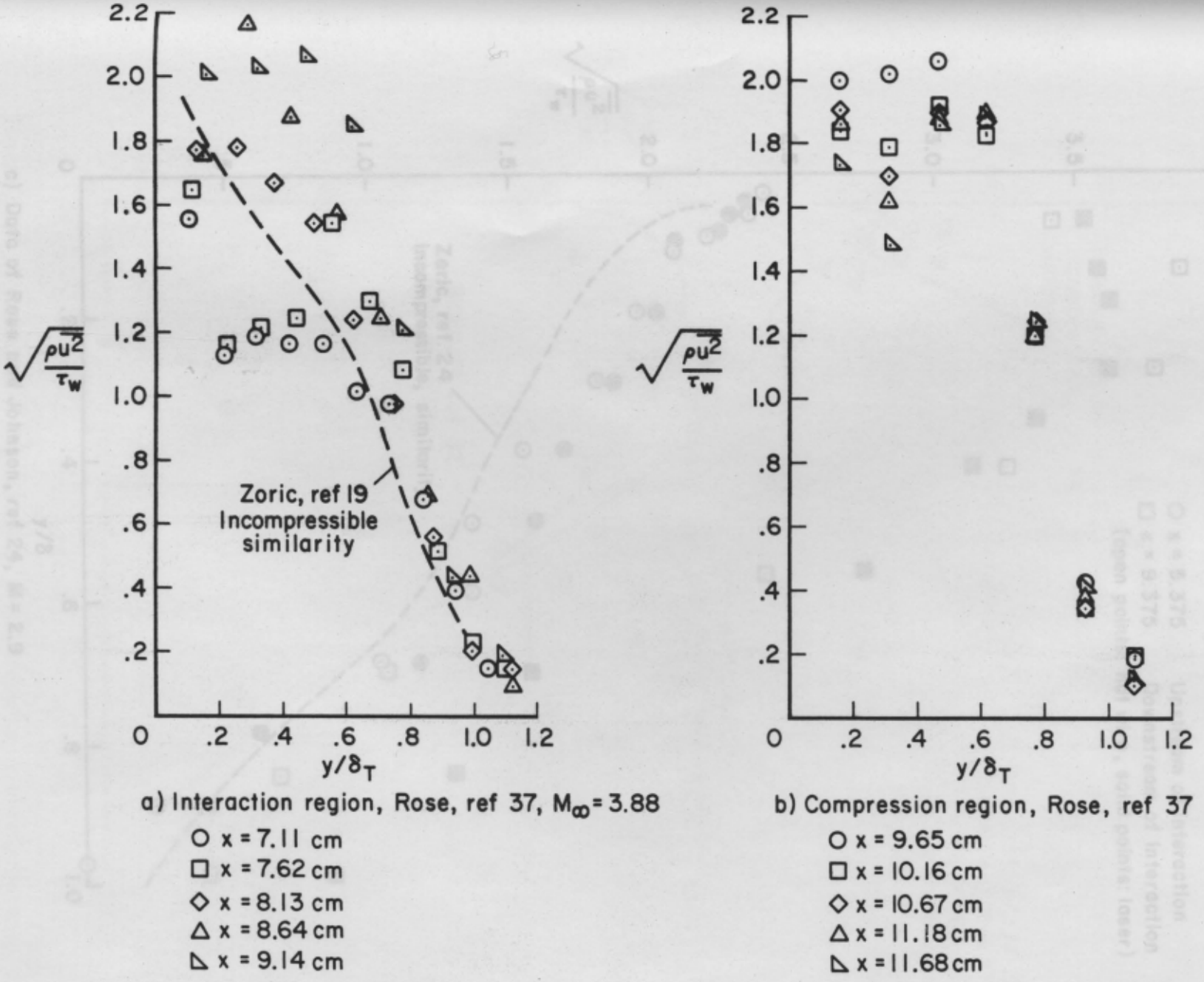

a) Interaction region, Rose, ref 37, $M_\infty = 3.88$

- ○ x = 7.11 cm
- □ x = 7.62 cm
- ◇ x = 8.13 cm
- △ x = 8.64 cm
- ◺ x = 9.14 cm

b) Compression region, Rose, ref 37

- ○ x = 9.65 cm
- □ x = 10.16 cm
- ◇ x = 10.67 cm
- △ x = 11.18 cm
- ◺ x = 11.68 cm

Figure 11.- Measurements of the longitudinal turbulent stress through shock-wave interactions.

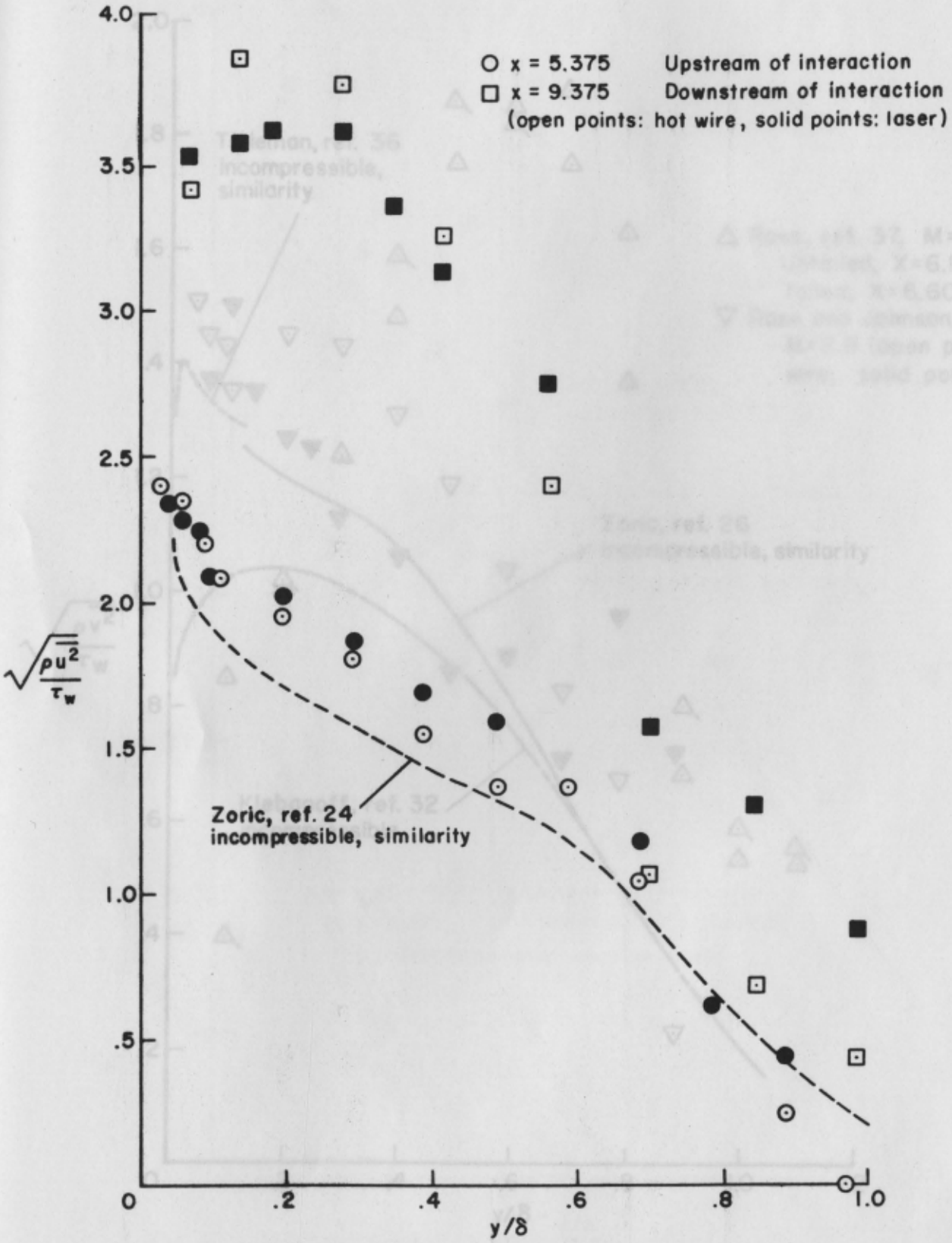

c) Data of Rose and Johnson, ref 24, M = 2.9

Figure 11.- (Concluded).

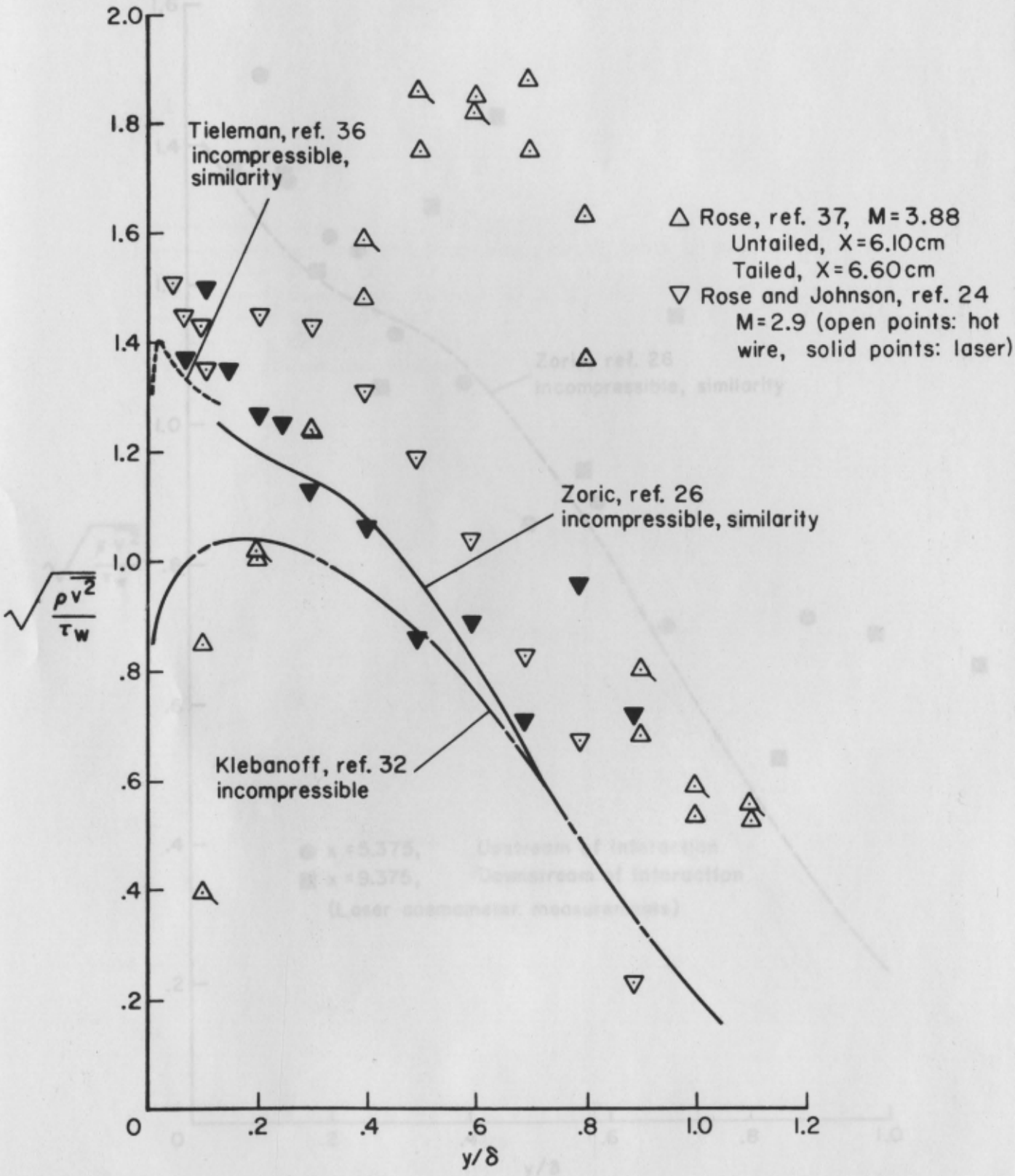

Figure 12.- Vertical turbulent velocity measurements in zero pressure gradient boundary layers.

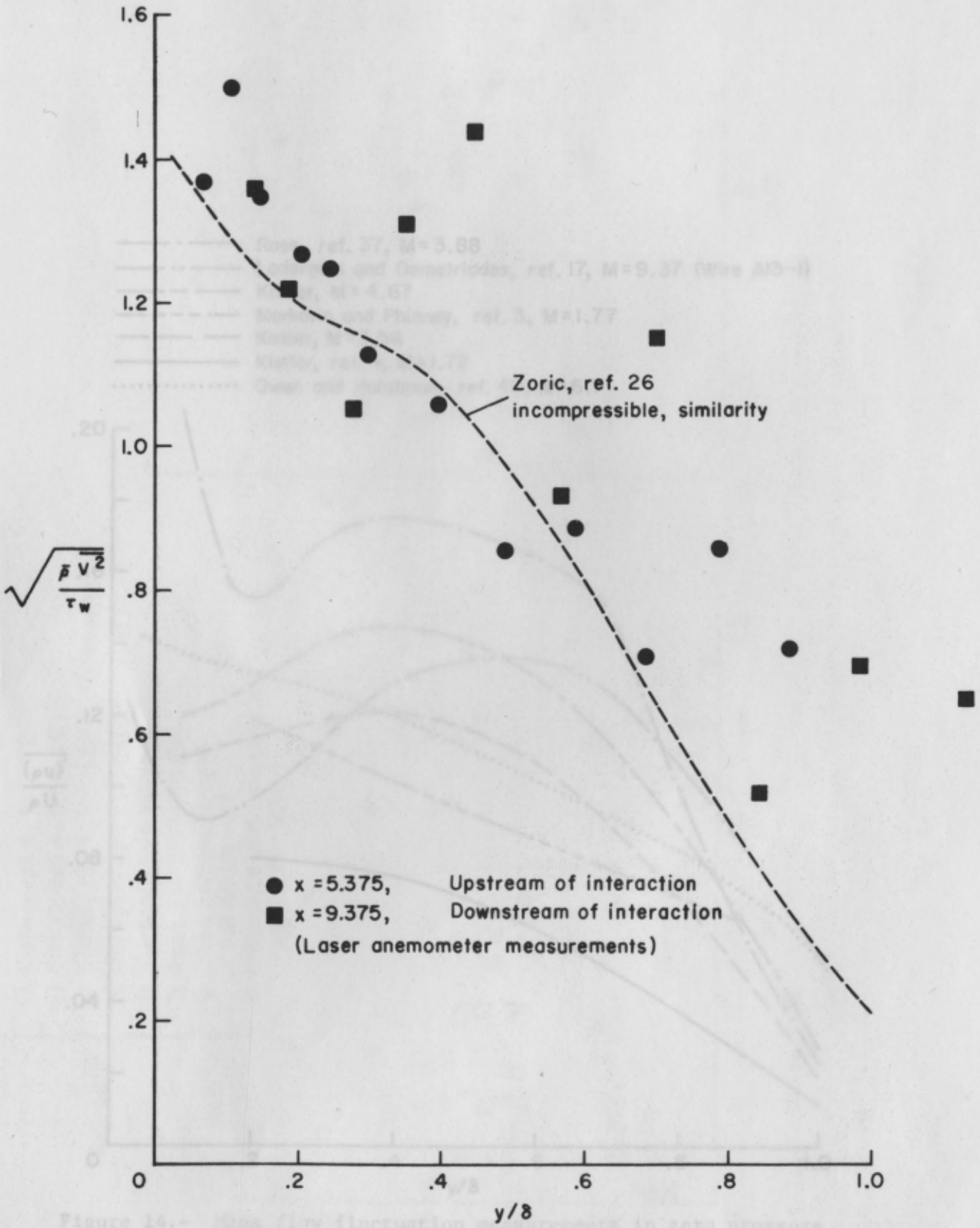

Figure 13.- Vertical turbulent velocity measurements through a shock-wave interaction.

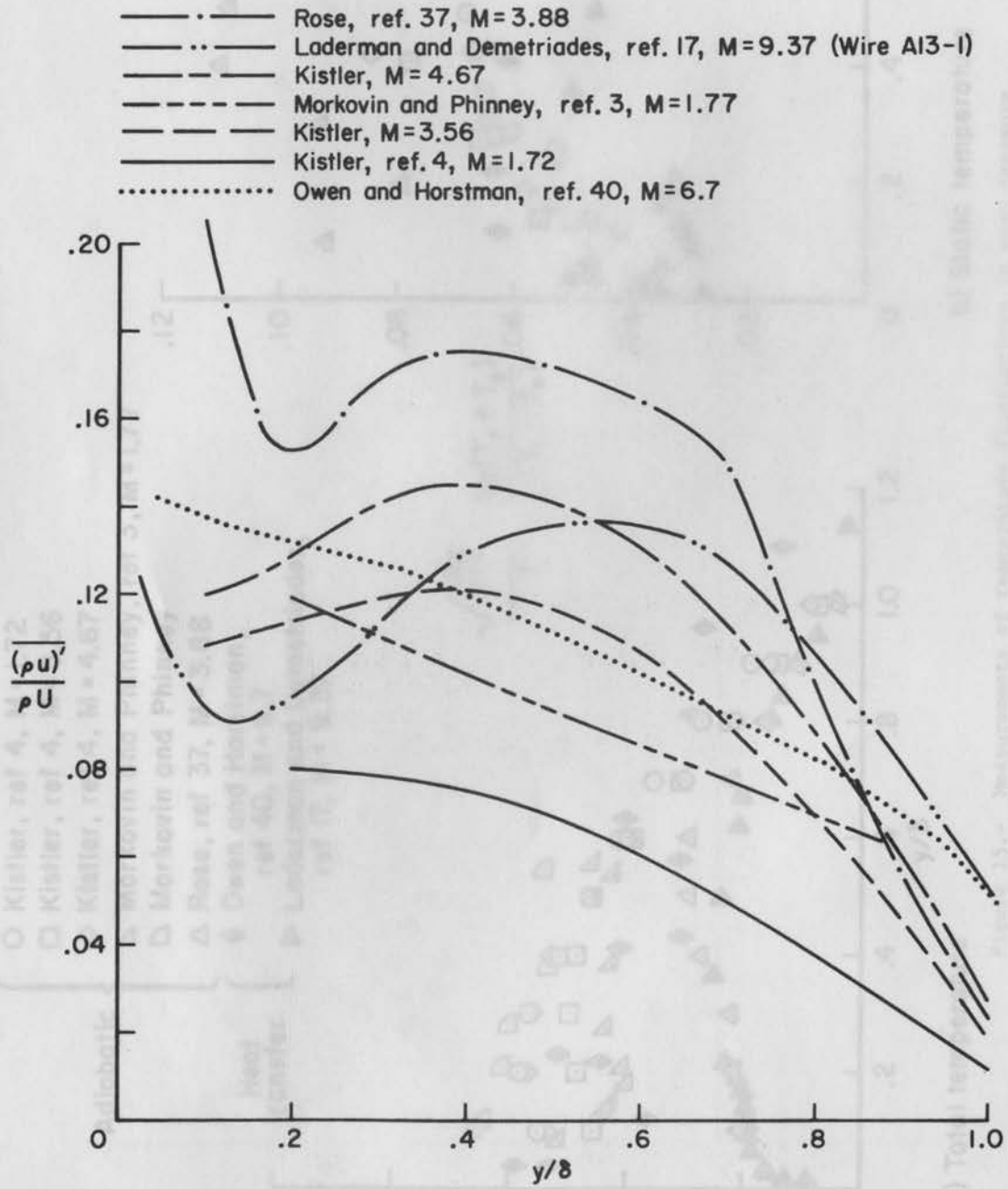

Figure 14.- Mass flow fluctuation measurements in zero pressure gradient boundary layers.

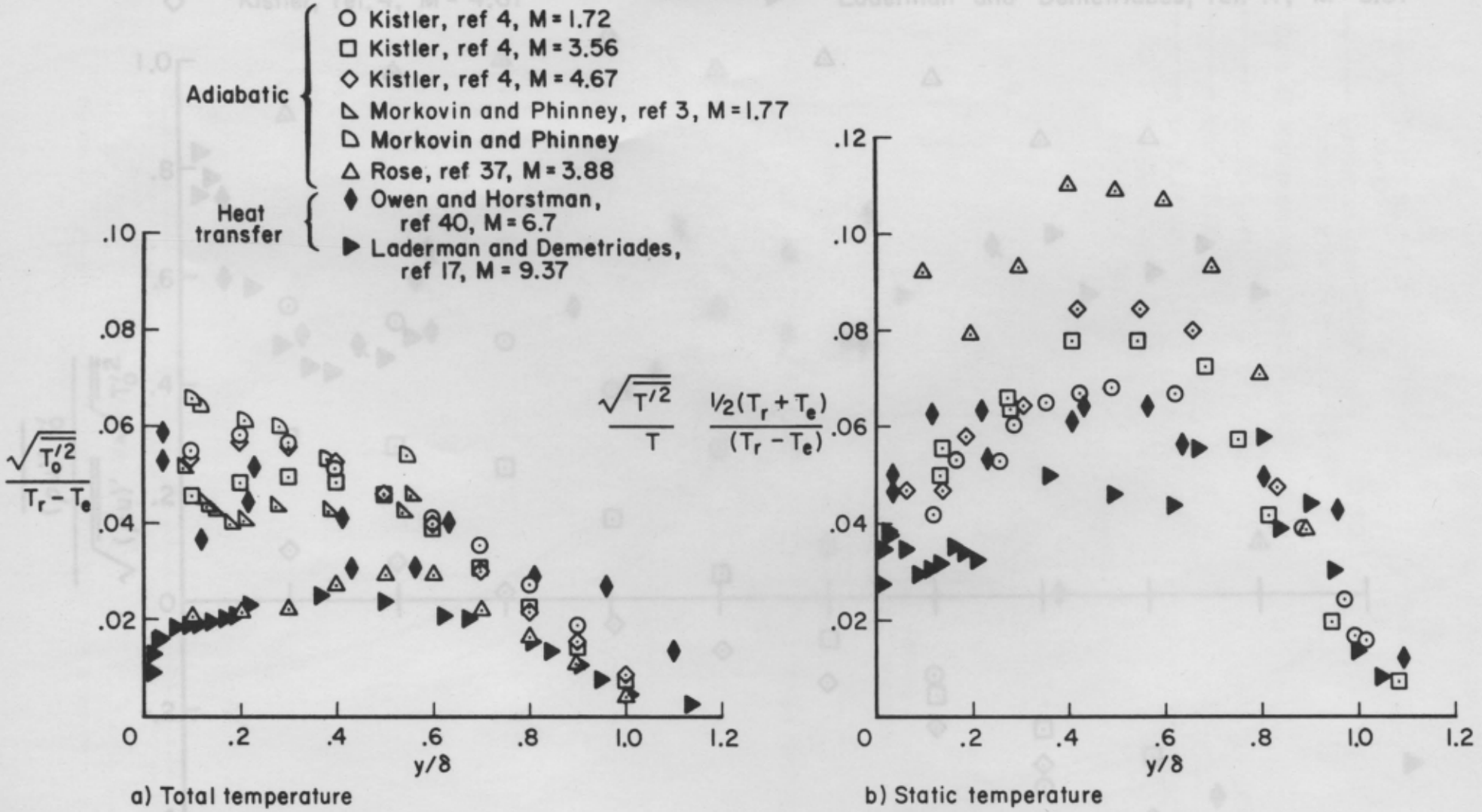

Figure 15.- Measurements of temperature fluctuations in zero pressure gradient boundary layers.

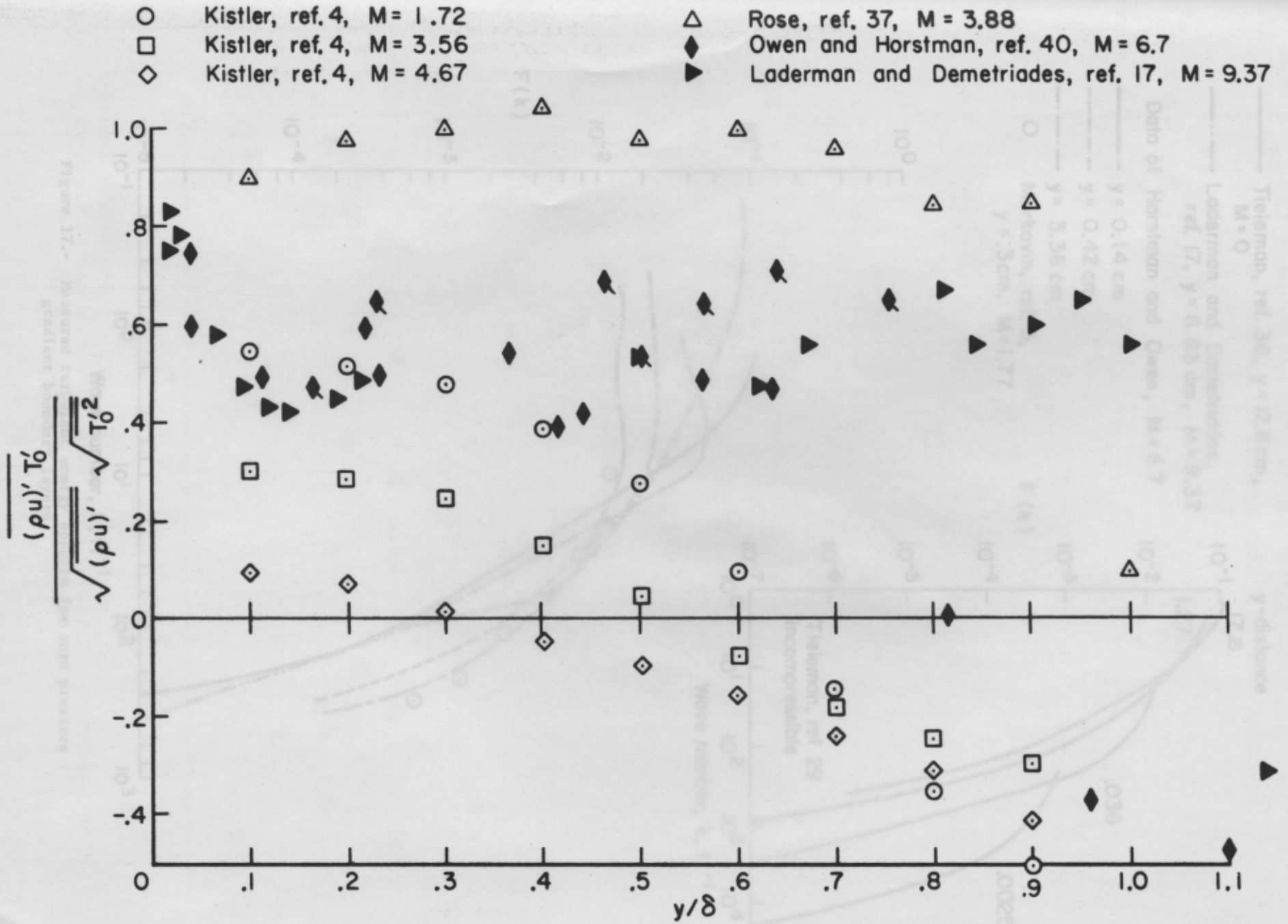

Figure 16. Measurements of the correlation between the mass flux and temperature fluctuations in zero pressure gradient boundary layers.

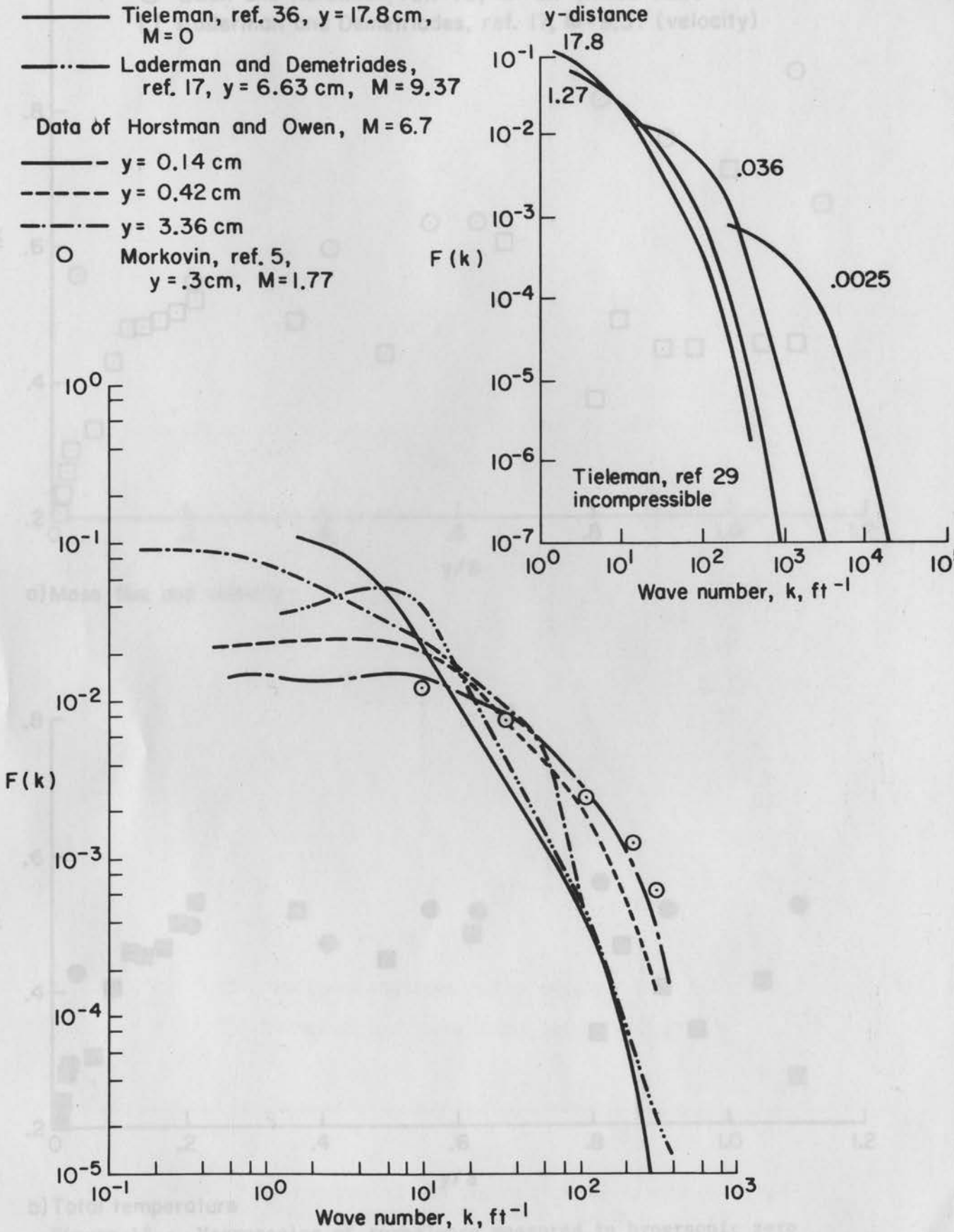

Figure 17.- Measured turbulent energy spectra for zero pressure gradient boundary layers.

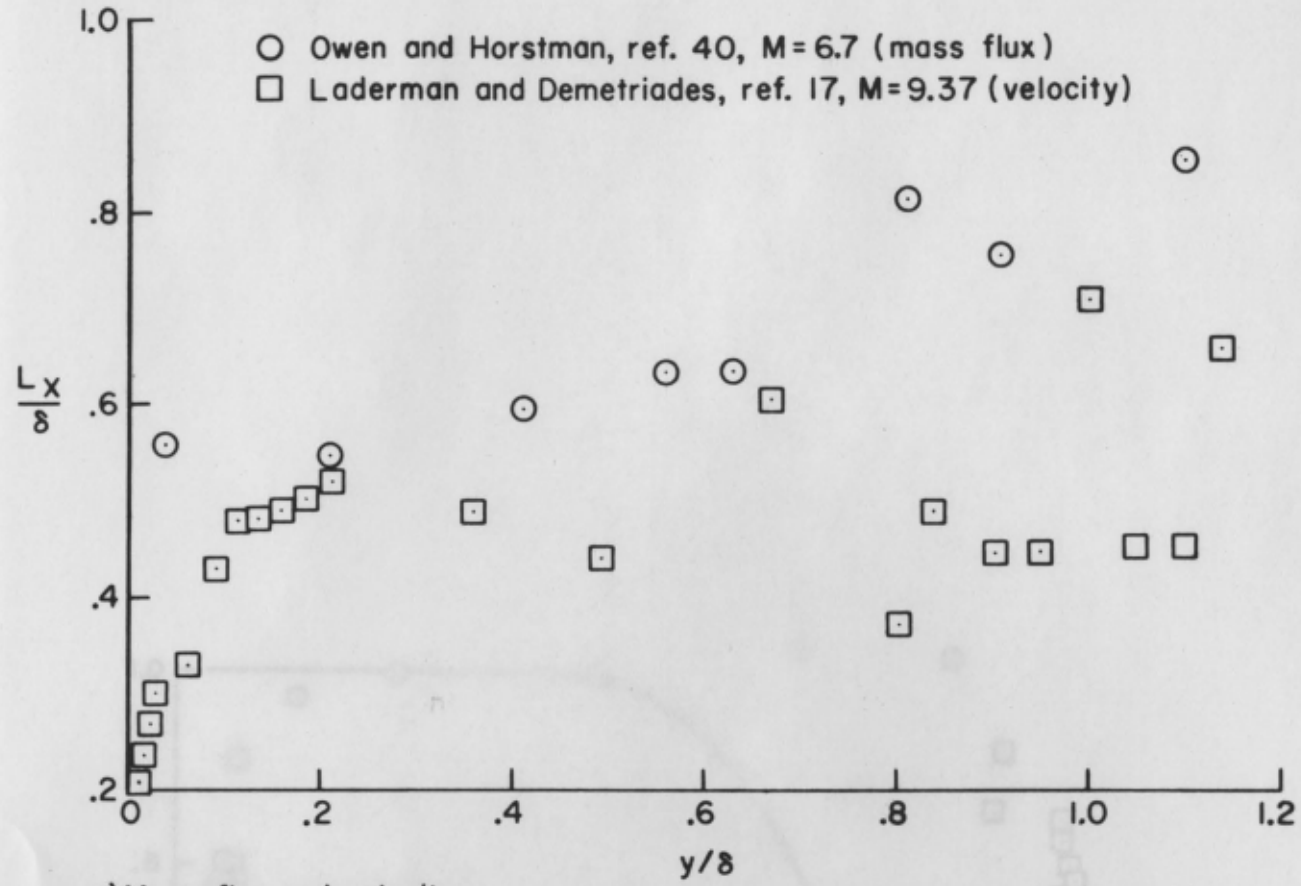

a) Mass flux and velocity

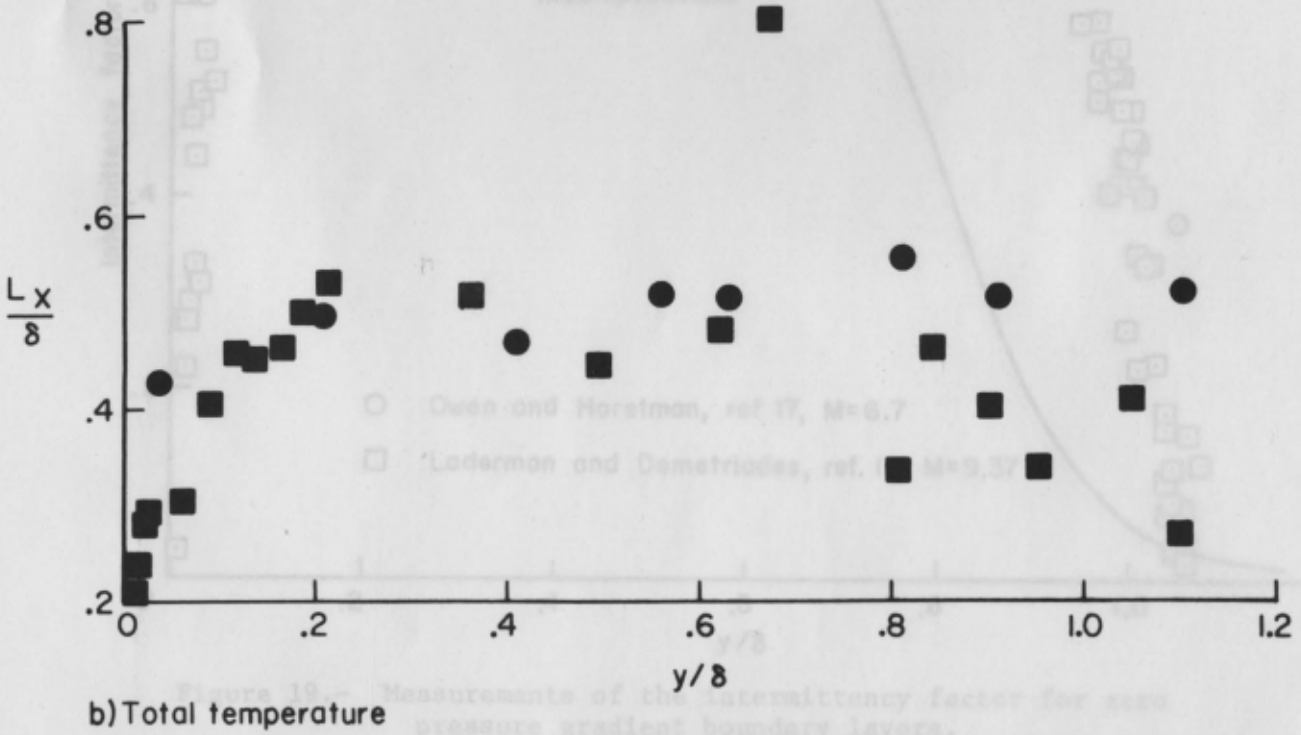

b) Total temperature

Figure 18.- Macroscales of turbulence measured in hypersonic zero pressure gradient boundary layers.

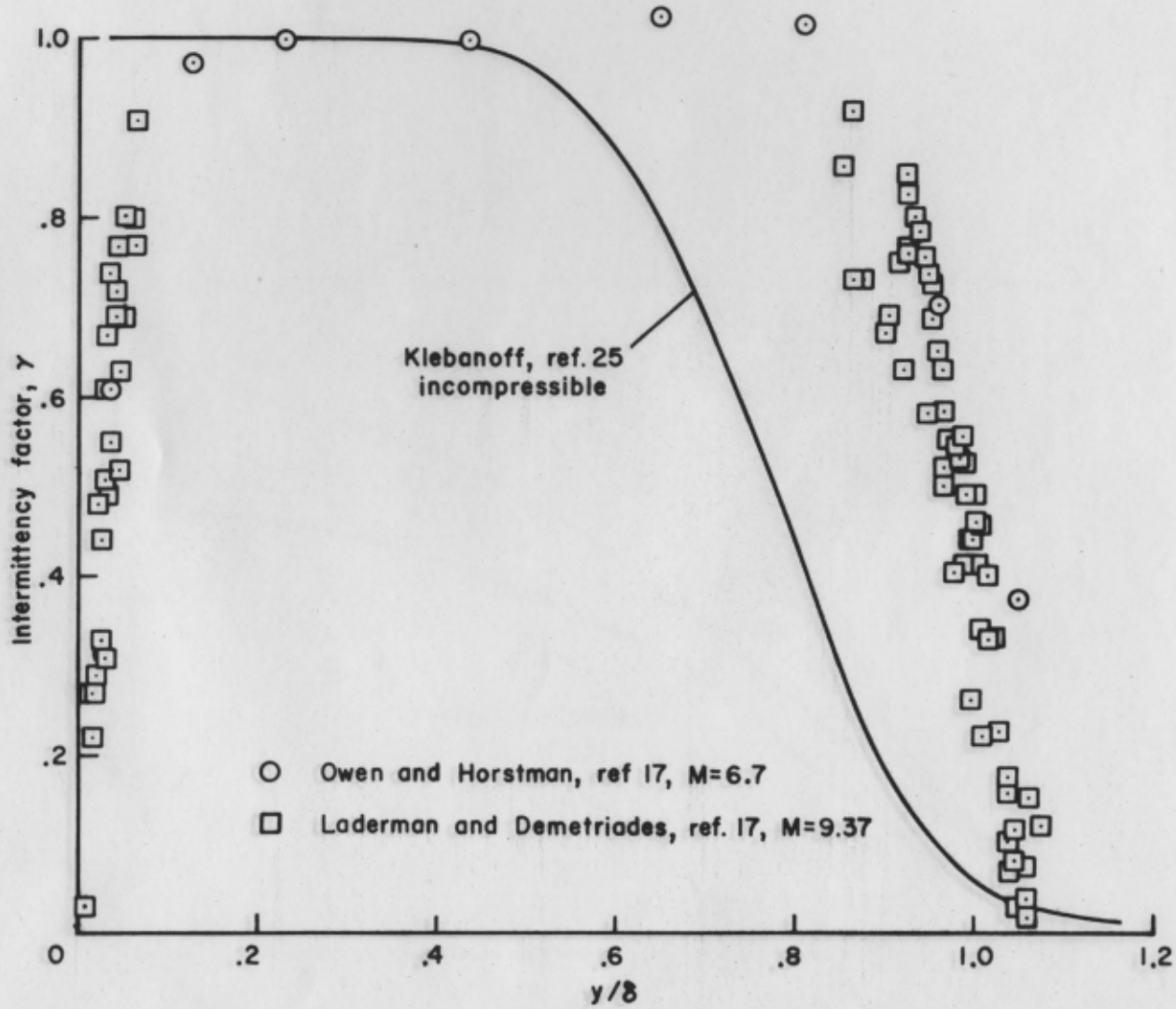

Figure 19.- Measurements of the intermittency factor for zero pressure gradient boundary layers.

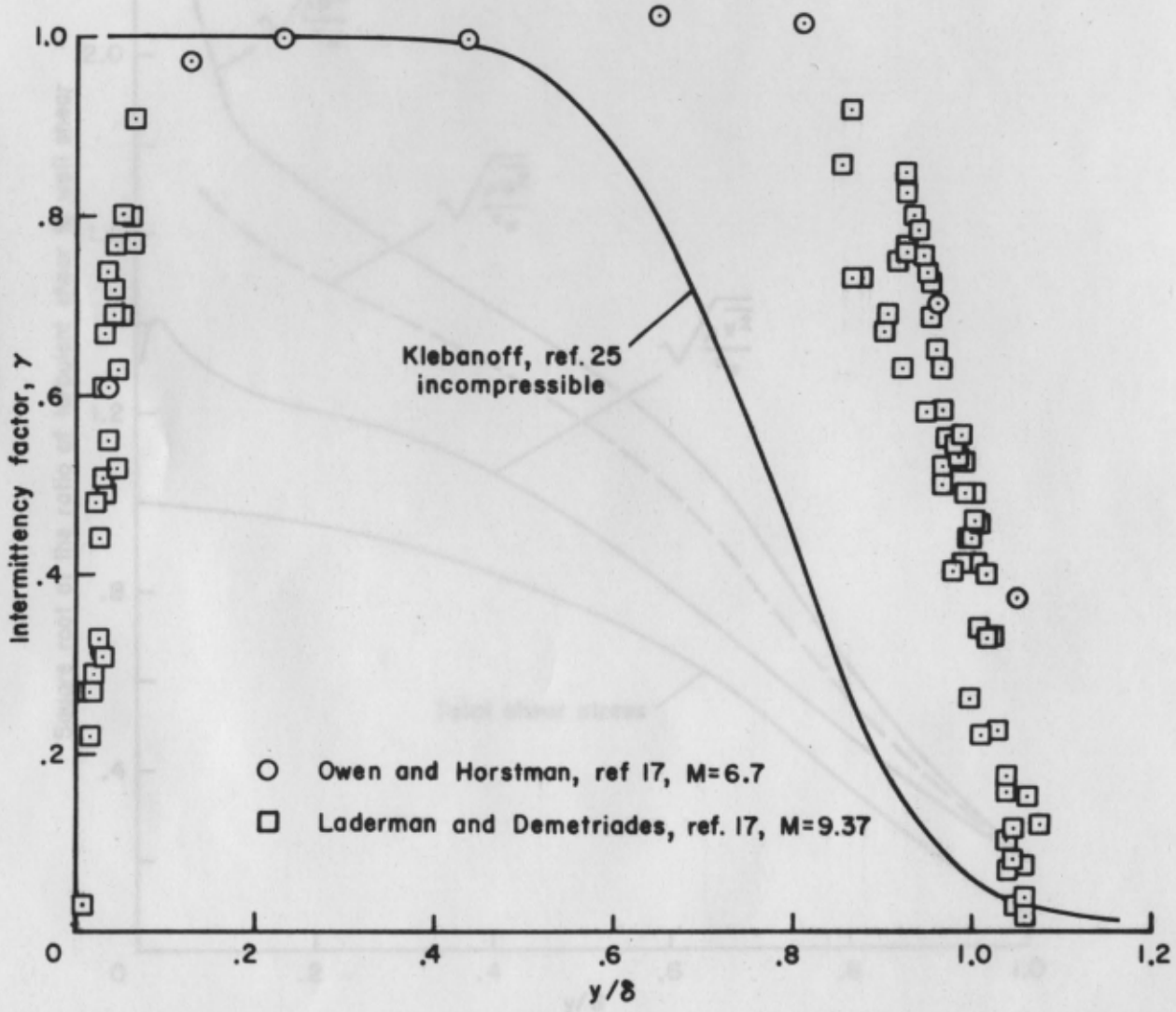

Figure 19.- Measurements of the intermittency factor for zero pressure gradient boundary layers.

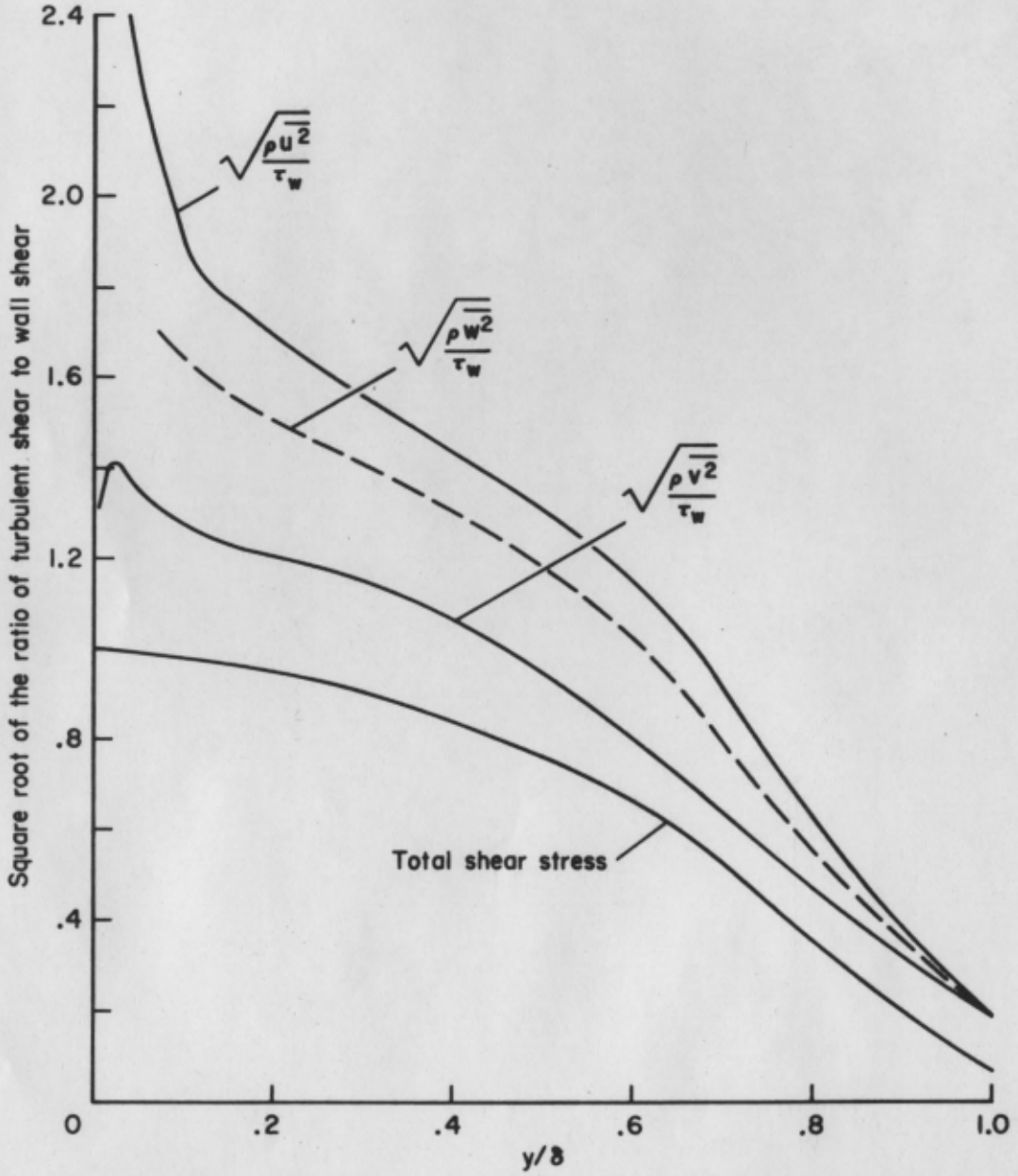

Figure 20- Values of the turbulent stress terms for large scale, zero pressure gradient, turbulent boundary layers.